Hydrol. Earth Syst. Sci. Discuss., 10, 3743–3794, 2013
www.hydrol-earth-syst-sci-discuss.net/10/3743/2013/
doi:10.5194/hessd-10-3743-2013

Hydrology and
Earth System
Sciences
Discussions
Open Access

Elevational dependence of climate change impacts on water resources in an Alpine catchment

S. Fatichi, S. Rimkus, P. Burlando, R. Bordoy, and P. Molnar

Institute of Environmental Engineering, ETH Zürich, Switzerland

Received: 7 March 2013 – Accepted: 8 March 2013 – Published: 20 March 2013

Correspondence to: S. Fatichi (simone.fatichi@ifu.baug.ethz.ch)

Published by Copernicus Publications on behalf of the European Geosciences Union.

Title Page
Abstract | Introduction
Conclusions | References
Tables | Figures
◀| |▶
◀ ▶
Back | Close
Full Screen / Esc
Printer-friendly Version
Interactive Discussion

Abstract

An increasing interest is directed toward understanding impacts of climate change on water related sectors in a particularly vulnerable area such as the Alpine region. We present a distributed hydrological analysis at scale significant for water management for pristine, present-days, and projected future climate conditions. We used the upper Rhone basin (Switzerland) as a test case for understanding anthropogenic impacts on water resources and flood risk in the Alpine area. The upper Rhone basin includes reservoirs, river diversions and irrigated areas offering the opportunity to study the interaction between climate change effects and hydraulic infrastructures. We downscale climate model realizations using a methodology that partially account for the uncertainty in climate change projections explicitly simulating stochastic variability of precipitation and air temperature. We show how climate change effects on streamflow propagate from high elevation headwater catchments to the river in the major valley. Changes in the natural hydrological regime imposed by the existing hydraulic infrastructure are likely larger than climate change signals expected by the middle of the 21th century in most of the river network. Despite a strong uncertainty induced by stochastic climate variability, we identified an elevational dependence of climate change impacts on streamflow with a severe reduction due to the missing contribution of water from ice melt at high-elevation and a dampened effect downstream. The presence of reservoirs and river diversions tends to decrease the uncertainty in future streamflow predictions that are conversely very large for highly glacierized catchments. Despite uncertainty, reduced ice cover and ice melt are likely to have significant implication for aquatic biodiversity and hydropower production. The impacts can emerge without any additional climate warming. A decrease of August-September discharge and an increase of hourly-daily maximum flows appear as the most robust projected changes for the different parts of the catchment. However, it is unlikely that major changes in total runoff for the entire upper Rhone basin will occur in the next decades.

1 Introduction

The Alpine region has been identified as an area particularly vulnerable to climate change in a series of sectors such as flood risk, water resources, ecological services, tourism (Koenig and Abegg, 1997; Theurillat and Guisan, 2001; Elsasser and Bürki, 2002; Zierl and Bugmann, 2005; Fuhrer et al., 2006; Beniston, 2006; Schädler and Weingartner, 2010; Viviroli et al., 2011; Rixen et al., 2011; Dobler et al., 2012; Beniston, 2012). The Alpine region of Switzerland has been, moreover, represented as the "water tower of Europe" (Viviroli et al., 2007; Beniston, 2012) since important rivers flowing through central (Inn, Danube), western Europe (Rhine) as well as toward the Mediterranean sea (Rhone, Po) originate from this region, which contributes an important fraction of their runoff, especially in summer months (Huss, 2011). Given the importance of the Alps for local and downstream water related activities, there is a pressing need from stakeholders and public managers for studies addressing implications of climate change on this area (Hill et al., 2010; Beniston et al., 2011). These studies are required to provide information on different characteristics of the flow regime such as amount, seasonality, minima and maxima, as well as estimates of other hydrological variables, e.g. soil moisture and snow cover. The presented research aims at refining and improving quantitative projections of changes in river flows in the upper Rhone basin and represents the driver for additional impact studies within the European large integrating project "ACQWA" (Assessing Climate change impacts on the Quality and quality of WAter) (Beniston et al., 2011).

The upper Rhone catchment constitutes a perfect test ground and an optimal example to investigate climate change impacts in the Alpine region since it includes most of the characteristics of Alpine mountain catchments, such as glacierized areas, a large range of elevations, the presence of river diversions and reservoirs for hydropower operations, and river intakes for irrigation. Furthermore, the upper Rhone is influenced by both Mediterranean and continental climate characteristics, making particularly interesting to study it in a changing climate (Beniston, 2012). For these reasons, several sub-catchments of the upper Rhone basin have already been the subject of studies of climate change effects on the hydrological regime (Zierl and Bugmann, 2005; Horton et al., 2006; Schaefli et al., 2007; Rössler et al., 2012; Uhlmann et al., 2012; Finger et al., 2012; Farinotti et al., 2012). These studies analyzed impacts of climate change at specific locations providing insights on the possible future hydrological regime and related vulnerabilities. They generally found a significant impact of climate change on runoff regime with a shift toward an earlier onset of snow melting in spring, a reduction of summer streamflow due to glacier retreat, and enhancing of dry conditions (Zierl and Bugmann, 2005; Rössler et al., 2012). Therefore, changes were found to negatively affect hydropower operations (Schaefli et al., 2007; Finger et al., 2012). However, given their focus on upper tributaries, they did not provide any general, distributed and cross-scale overview of changes in the entire upper Rhone basin. Even studies that used distributed hydrological models analyzed effects at the catchment outlet or in a specific reservoir only (Finger et al., 2012). However, the spatial scale at which water managers and policy makers are requested to take decisions is the scale of the upper Rhone river basin. Local changes are important but they need to be identified throughout the entire basin.

In order to provide an answer to such a request, this study presents a distributed investigation of the propagation of climate change effects on streamflow from the headwater catchments at high elevation to the main streams in the valleys at lower elevations. We are specifically interested in understanding if the effect of climate change on the streamflow regime has an elevational and stream order dependence and if there are significant geographical differences within the upper Rhone basin. Existing studies are strongly biased toward high-elevation catchments mostly fed by glacier sources. These studies focus on catchments that are not influenced by anthropogenic infrastructures, so that they can use their streamflow observations for calibration of hydrological models that simulate the natural flow regime. We argue that results obtained from these studies might provide a limited perspective whereas a more balanced approach to climate change impacts in mountainous catchments should be based on a larger scale and fully distributed analysis that is the goal of this study.

A significant part of the upper Rhone basin river network is highly regulated through river diversions and reservoir storages, which make an accurate hydrological modeling particularly challenging and require the inclusion of these infrastructures and of their operations. This represents a challenge as testified by an almost complete lack of publications in which the hydrology of the entire upper Rhone catchment is simulated (see for an exception Meile et al., 2011), especially compared to the numerous studies for small undisturbed tributaries. Because the technical data of existing infrastructure are not always available, we adopted a very pragmatical engineering approach for simplifying the representation of hydraulic infrastructures whenever this was the case. Numerical simulations were performed with the hydrological model Topkapi-ETH, that is a substantial evolution of the original rainfall-runoff model Topkapi (Ciarapica and Todini, 2002; Liu and Todini, 2002) and of successive updates (e.g. Finger et al., 2012). The model was modified for running long-term hydrological analysis in complex topographic environments and to explicitly account for anthropogenic influences. Despite several simplifications, we demonstrated that the adopted methodology provided highly satisfactorily results once the performance of the hydrological model was tested in reproducing present day (1990–2008) and natural flow regimes (before 1950). The upper Rhone basin offers a singular opportunity to evaluate model simulations in reproducing both natural and regulated flows because discharge observations were available at a few streamgauges from the beginning of the 20th century, i.e. before reservoirs and river diversions were constructed. Simulations of natural and regulated flows also allow us to quantify in detail, for the first time, the anthropogenic impact induced by the presence of infrastructure and to compare it with modifications induced by climate change. The presence of hydraulic infrastructure and their operations are assumed unmodified for simulations of future climate, in order to isolate the effects of climate change from any adaptation imposed by altered energy market or demand. The interaction of climate change with the existing hydraulic infrastructure provides a novel and important perspective in climate change impact studies.

In order to simulate future climate scenarios at the catchment scale, climate model realizations have to be transferred to spatial and temporal scales suitable for hydrological modeling. We used a combination of dynamic and stochastic downscaling. Realizations from three climate models, one Global Climate Model (GCM), ECHAM5, and two Regional Climate Models (RCMs), REMO and RegCM3 driven by ECHAM5 were used to derive factors of change for different climate statistics. The factors of change were derived independently for each decade from 2011 to 2050, using the period of 1991 through 2010 as control scenario period. Successively, they were used as input into a stochastic downscaling procedure (Bordoy, 2013; Bordoy and Burlando, 2013c). Each future decade and the control scenario were assumed stationary. We limited the analysis to A1B emission scenario (IPCC, 2000), however, since future climate simulations are limited to the year 2050, the choice does not represent a serious limitation because all of the emission scenarios are very similar for the first half of the 21th century (Hawking and Sutton, 2009; Prein et al., 2011).

We acknowledge that using only one GCM and two RCMs can significantly underestimate the uncertainty of climate change projections, since the variability among model realizations is considered as one of the principal source of uncertainty (Déqué et al., 2005; Räisänen, 2007; Knutti, 2008; Christensen et al., 2010; Hawking and Sutton, 2011). However, the stochastic downscaling approach allows us to alleviate the underestimation of uncertainty induced by neglecting realizations from additional climate models. Stochastic downscaling methodologies fully account for the uncertainty imposed by the internal variability (stochasticity) of the climate system (Burton et al., 2010; Fatichi et al., 2013). A recent analysis of a GCM has demonstrated that internal climate variability can account for more than half of the spread of the CMIP3 multi-model ensemble for several climatic variables, and gives a comparable variability for precipitation (Deser et al., 2012). Another stochastic downscaling methodology showed that climate stochasticity for precipitation is likely to cover a large fraction (although not all) of the uncertainty generated by considering a multi-model ensemble (Fatichi et al., 2013). Therefore, we assume that despite the fact that we are considering only three climate models (or just one if we refer to the driving GCM), the stochastic variability will account for a significant fraction of uncertainty of climate change projections for the upper Rhone basin.

2 Material and methods

2.1 Hydrological model

Hydrological simulations were performed with a significantly enhanced version, Topkapi-ETH, of the TOpographic Kinematic APproximation and Integration model, Topkapi, which was first introduced as a rainfall-runoff model by Ciarapica and Todini (2002); Liu and Todini (2002). The model uses a grid based representation of topography and a vertical discretization of belowground in three layers. The first two layers represent shallow and deep soil horizons and are schematized as non-linear reservoirs, the third layer is schematized as a linear reservoir useful to mimic the behavior of slow-flow components such as porous or fractured rock aquifers. Grid elements are connected in the surface and in the subsurface according to topographic gradients. A kinematic approximation is used to route subsurface, overland, and channel flow (Liu and Todini, 2005). Potential infiltration rate is regulated by an empirical equation and runoff might result from infiltration or saturation excess processes. Incoming shortwave radiation at the surface is mediated by local and remote topographic effects as described in Corripio (2003). Topographic effects on radiation are particulary important in mountainous terrains. Potential evapotranspiration is calculated using the Priestly-Taylor equation (Priestley and Taylor, 1972; Brutsaert, 2005), in which net radiation is assumed to be only a function of incoming shortwave radiation, albedo, and air temperature through an empirical equation (Rosso, 2000). A monthly correction factor is applied to evapotranspiration to distinguish between different land uses. Snow and ice melt are calculated with an empirical enhanced temperature index model, which requires air temperature and shortwave radiation only (Pellicciotti et al., 2005; Carenzo et al., 2009). Liquid precipitation and snow/ice melt in a glacier are stored in a linear reservoir to simulate the time-lag between actual percolation in ice moulins and crevasses and glacier outflow.

While Topkapi-ETH does not have the richness and rigorousness of process representation of physically-based state-of-the-art hydrological models (Ivanov et al., 2004; Rigon et al., 2006; Kollet and Maxwell, 2006; Ivanov et al., 2008; Ebel et al., 2008; Shen and Phanikumar, 2010; Camporese et al., 2010; Fatichi et al., 2012a,b), it represents a reasonable compromise between physically meaningful representation of hydrological processes and computational time for large-scale, long-term, high-resolution, distributed simulations. We specially considered the preservation of high-resolution topography to be an asset for hydrological simulations in complex terrain such as the upper Rhone basin. Additionally, fast computational times are required by the chosen stochastic approach for climate change simulations.

Furthermore, when compared to other models, Topkapi-ETH offers the opportunity to include and simulate a range of anthropogenic infrastructure and management activities (e.g. reservoirs, irrigation) that interact significantly with the natural hydrological cycle and that are essential for providing simulations in the regions of major interest for the society. Specifically, lakes and reservoirs are described using all of the major technical information, e.g. spillway, turbine and outlet capacity, volume-level curves, maximum and minimum regulation levels, environmental flows. Different operational rules can be implemented for reservoirs, but in this study a target level rule is specified as described in Sect. 2.2. River diversions are simulated defining intake and return points, diversion capacity and efficiency. One hour lag is used to transfer water through the diversion regardless of the traveled distance, being the latter typically unknown. Water withdrawals due to irrigation or domestic/industrial water use can be specified in selected channels, aquifers or lake grid points. Withdrawals for irrigation are triggered when soil moisture in certain pre-defined irrigation areas and periods decreases below a critical threshold. Independently from the actual agricultural needs, for each withdrawal point, water for irrigation cannot exceed a given maximum value fixed by the physical infrastructure (irrigation channels, pipes). Domestic/industrial uses are supplied with specified withdrawal functions that are based on the number of inhabitants and follow pre-defined seasonality and intrannual variability of water consumption. Water is given back to the river network with a time lag and after a fixed fraction of losses is subtracted.

2.2 Study area, data, and modeling assumptions

The upper Rhone basin is located in the south-west corner of Switzerland (Latitude, 46.2° N, Longitude, 7.6° E of the barycenter coordinate). It originates at the outlet of the Rhone glacier and flows into the Lake Geneva after the streamgauge of Port du Scex (Fig. 1). The total drained area is 5338 km^2 and elevation ranges from 377 to 4634 m a.s.l. Precipitation and air temperature averaged over the entire catchment in the period October 1990 through December 2008 are 1400 $\mathrm{mm\,yr}^{-1}$ and 1.86 °C, respectively.

2.2.1 Climate forcing

Meteorological data required by Topkapi-ETH are hourly values of precipitation, air temperature, and daily cloud transmissivity for each computational element in the catchment. Hourly observations of precipitation, air temperature and shortwave incoming solar radiation were available for the period October 1990 through December 2008 for 9, 16, and 12 stations, respectively, without significant data gaps (Fig. 1). Gridded daily precipitation at $2\times2\,\mathrm{km}^2$ resolution was also available as elaborated product, RhiresD, of Meteo Swiss (Schwarb, 2000; Wuest et al., 2010). Precipitation inputs to each computational element of the model were assigned on the basis of the RhiresD product disaggregated from daily to hourly resolution according to the timing of precipitation observed at the stations. Specifically, the nearest station was used to define the hourly partition of the daily precipitation contained in RhiresD. In case of precipitation larger than zero only in the gridded product, a uniform precipitation was assumed for a duration of 7 h, that corresponds to the typical duration of precipitation during a rainy day, according to the available data. The use of RhiresD gridded product as precipitation input results in about 400 mm yr^{-1} more than precipitation obtained with classical interpolation methods from at station data (e.g. Thyssen polygons or Inverse Distance Weighting). This represents a much more realistic precipitation forcing for the upper Rhone area. Station observations of air temperature were interpolated using Thyssen polygons and assuming a constant air temperature lapse rate of 5.5 °C km^{-1} estimated as the best fit obtained from the available data. Observed values of shortwave radiation were compared with clear sky shortwave radiation simulated using the weather generator, AWE-GEN, (Fatichi et al., 2011), in order to estimate values of cloud transmissivity for each station and hour of the day with non-zero radiation. A single time series of daily cloud transmissivity is then calculated for the entire catchment as the average of the multiple stations and diurnal hours.

2.2.2 Topography, land cover and soil

Topographic data were obtained resampling a fine resolution (25×25 m^2) Digital Terrain Model (DTM) of Switzerland to 250×250 m^2 resolution. This produces in total 85409 computational elements. Land use information were derived from the Global Land Cover Product (GlobCover) (2005–2006) and resampled from 300×300 to 250×250 m^2 resolution. Correction to GlobCover were made on the basis of additional available maps for lakes and glaciers. A soil map of Rhone at 500×500 m^2, provided by the Swiss agronomic research institute “Agroscope” was used to assign soil properties distributed in space. These include residual and saturated water content, vertical hydraulic saturated conductivity and soil-pore size distribution index. Rocks and terrain below glaciers were treated as a special category of “soil” with only the third subsurface layer of Topkapi-ETH (linear reservoir) used to approximate fractured rock aquifer dynamics.

2.2.3 Glaciers

Glacier cover in the entire catchment was assigned based on the GLIMS Glacier Database (Fig. 1). In total, 617 km^2 or 11.5 % of the catchment was classified as ice covered, this leads to 183 different glacier units, including large (> 10 km^2) glaciers such as Aletschgletscher or Rhonegletscher and glaciers occupying a single grid cell. An assumption was made regarding the initial conditions of ice thickness in the glaciers. For each glacier, we derived the total volume using an empirical function of the projected area, A [km^2] (Bahr et al., 1997; Farinotti et al., 2009b) and then we assumed a uniform thickness, h_{Ice} [m] for each glacier dividing the volume by the area, i.e. $h_{\mathrm{Ice}} = 33A^{0.36}$. Such a simplification was a necessary compromise to specify ice thickness conditions for all of the glaciers in the basin, since distributed information of ice thickness was available for a few glaciers only and affected by a large uncertainty (Bauder et al., 2007; Farinotti et al., 2009a). Initial ice thickness was required to successively simulate the potential retreat of glaciers due to melting.

2.2.4 River diversions and reservoirs

Information on river intakes and returns were taken from the detailed product “Restwasserkarte” available from the Swiss Federal Office for the Environment (BAFU). Specifically, the coordinates together with estimates of the mean monthly diverted quantity were available for the major river intakes and returns. The capacity of the diversions was assumed to be the highest monthly withdrawn discharge and efficiencies of the diversions were always assumed to be equal to one. Conduits from the dams to the hydropower plants and pumping pipes were also included as part of the river diversion network. Their capacity was given on the basis of conduits or pumping system capacities whenever this information was available (Jordan, 2007). In total, 115 diversions/conduits were included manually in the model to check consistency between coordinates of intake/return points and the modeled river network. These include all the recorded diversions that had a capacity larger than 0.1 m^3 s^{-1}, including 4 intakes that divert water outside of the upper Rhone basin. Such a large amount of disturbances is related to the hydropower activity occurring in the upper Rhone basin. Water is collected in different valleys and transported to the major reservoirs and/or directly into the network of conduits that supply the hydropower plants (Fig. 2). While carefully implemented, the simulated scheme is only a coarse approximation of the complex reality and it represents our best effort to consider anthropogenic alterations of the natural discharge of the upper Rhone river basin given the limited availability of public data.

Along with river diversion the major anthropogenic disturbance is given by the operation of large reservoirs. We explicitly simulated 14 reservoirs with volume capacity ranging from $6.49 \times 10^6\,\mathrm{m}^3$ of Illsee to the $400 \times 10^6\,\mathrm{m}^3$ of Lac des Grande Dixence, that represents the largest reservoir of the European Alps (Fig. 2). One of the reservoir, Arnensee, is not physically located in the Rhone catchment but since discharge from Rhone tributaries is pumped back and forth from its reservoir, it is explicitly included in the simulation. Dams were mostly built between 1950 and 1970 leading to a total storage capacity of almost $1.2\,\mathrm{km}^3$ that represents 20 % of the total annual upper Rhone flow (Loizeau and Dominik, 2000). Fundamental technical information about the dams, such as maximum storage volume, maximum and minimum regulation levels, flood maximum level, maximum outflow capacity through normal outlets, bottom outlets, and spillway were taken from the archive of the "Swiss Committee on Dams". Volume-level curves and time series of levels were only available for seven reservoirs (including Mattmarksee and Griessee) of the broader alpine region at the boarder between Switzerland, Italy and France. Available volume-level curves representing the topographic shape of the reservoirs were normalized using the maximum and minimum regulation levels and averaged to obtain a reference normalized volume-level curve. This curve was then used to infer volume-level curves for the other reservoirs assuming that their valley topographies are similar. In the model, dams were operated according to a target-level policy. Specifically, a target level was assigned for each reservoir and for each day of the year. In case the actual simulated reservoir level exceeded the target level, water was released from the reservoir at a rate lower or equal to the outlet/intake capacity of the given dam. In case the simulated reservoir level was lower than the target level only the environmental flow was released. Above the maximum regulation level, the dam spillway is also considered as a way of releasing water. Target levels were derived from observations as long-term averages of reservoir levels for a given day of the year. For reservoirs where we did not have time series of levels, target levels were derived calculating a normalized target level from observations in the other reservoirs and multiplying this normal target level for the maximum minus minimum regulation level of the given reservoir. This simplification implies that all of the reservoirs in the Rhone catchment are simulated to operate in a similar way. Given the geographical proximity, the similar elevation (between 1700 and 2400 m a.s.l.) and their common use for hydropower production the assumptions can be considered to be rather realistic, although the different storage capacity of the reservoirs can lead to different management policies that we were not able to account for.

2.2.5 Irrigation and water consumption

The extent of areas the can be irrigated was defined on the basis of the land cover, since detailed data on irrigated areas were not available. A map identifying the agricultural areas was provided by the Swiss Federal Office for the Environment. All the agricultural areas were assumed to be potentially irrigated, although that is likely to represent an overestimation of the actual irrigated area. In total, fourteen irrigation districts were considered. The period when irrigation can be activated was assumed to be from April to September. The maximum capacity of the water supply infrastructure was assumed to be equal to $0.7\,\mathrm{mm\,h^{-1}}$ on the basis of the few available data. Identification of withdrawal points for irrigation is in reality rather complex due to the widespread system of irrigation channels, called “Suonen”, draining water from many small tributaries. As a simplification, in the model for each irrigated district water is withdrawn from the nearest upstream channel. The water used for irrigation in the simulation period 1990–2008 is equal to $160 \times 10^6\,\mathrm{m^3\,yr^{-1}}$, that is 60 % larger than an estimate available for the year 2006 for the entire Valais region (a region almost overlapping with the upper

Rhone basin). Given all the involved necessary assumptions this result can be considered acceptable and is unlikely to represent a limitation in the assessment of climate change impacts. From our calculations, water used for irrigation is indeed less than 3 % of the outflow from the watershed, although it can be more relevant at the local scale.

Domestic/industrial water consumption was calculated on the basis of demographic maps. A water allocation of 300 $\mathrm{L\,person^{-1}\,day^{-1}}$ was assumed for the entire area, as an estimate of combined domestic and industrial uses. Population was aggregated in units to limit the water withdrawal points. Specifically "withdrawal units" cannot host more than 20 000 inhabitants and cannot include inhabitants that are more than 5 km distant. This ensures that mountain villages are treated as separate units and that cities have several withdrawal points. In total, 68 units were identified, water was withdrawn from the deep subsurface layer (e.g. groundwater) for small communities, and from the closest channel point for larger communities. These are unavoidable assumptions given the fact that the actual withdrawal sources are heterogenous and largely unknown. Daily and seasonal fluctuations of water demand were imposed using modulation coefficients (Milano, 1996). Note that this cannot accommodate peak demands in mountain resort due to tourism or water used for artificial snow making. Under these assumptions, the simulated domestic/industrial water consumption in the period 1990–2008 was on average 0.98 $\mathrm{m^3\,s^{-1}}$, which represents less than 1 % of the outflow from the watershed.

2.3 Model calibration

Given the overall complexity of the upper Rhone river basin that includes hydrological processes occurring over 4000 m of elevation range and numerous hydraulic infrastructures, no automatic calibration was sought. We considered that, given the strong anthropogenic disturbances, automatic calibration could have led to identify parameter combinations that would rather compensate for approximations in the description of the system (river diversion, reservoirs) than represent the best parameter set for the specific case. Following the reasoning presented in Fatichi et al. (2012b), we also believe that calibration of physically-based models or models such as Topkapi-ETH where most of the parameters have a physical meaning, should represent the final tuning of a carefully implemented set-up, rather than the driver of model performance. We think that small improvements of metrics of performance obtained with combinations of parameters that are non consistent with the "expected" values, should be looked suspiciously. This is especially the case for climate change studies where the objective is not only the overall performance for present day climate but a correct representation of the processes. Therefore, few (< 15) manual adjustments were carried out after the original model set-up was prepared from available data. Specifically, we modified values of soil depth for the first two soil layers, values of vertical and horizontal saturated hydraulic conductivity, the parameters controlling the melting processes, and the correction factors for evapotranspiration. These parameters were modified to better reproduce the overall partition between evapotranspiration and runoff throughout the catchment, the melting period, winter minimum flows, and the summer/fall peak flows.

2.4 Generation of current and future climate forcing

Meteorological forcing variables representative of the future climate were obtained using a stochastic downscaling methodology (Burlando and Rosso, 1991, 2002; Burton et al., 2010; Bordoy, 2013; Bordoy and Burlando, 2013b). The downscaling methodology is based on two stochastic models for simulating hourly multi-site precipitation and air temperature that are assumed uncorrelated. Specifically, precipitation is simulated using the spatiotemporal Neyman-Scott Rectangular Pulses model implemented in the RAINSIM package (Burton et al., 2008). Air temperature is modeled with a multivariate Markovian model. Station observations for the control scenario 1991–2010 were used to parameterize these models for the present climate.

Climate change forcing is derived from climate model simulations in the form of factors of change (Fatichi et al., 2011; Anandhi et al., 2011). We used realizations for the period of 1991 through 2050, emission scenario A1B, from one Global Climate Model (GCM), ECHAM5 (Roeckner et al., 2003), and two Regional Climate Models

(RCMs), RegCM3 (Pal et al., 2007) and REMO (Jacob et al., 2007), both externally forced with ECHAM5. Factors of change were calculated comparing climate model simulated statistics in the 1991–2010 period with later decades. Since the focus of the ACQWA project is the future up to 2050, differences due to emission scenarios are considered of minor importance and therefore neglected. Factors of change are computed for precipitation and air temperature statistics after applying a bias correction procedure (Bordoy and Burlando, 2013a). Differences between station observations and climate model simulations in the control scenario (1991–2010) are corrected through a non-linear parametric method (Leander and Buishand, 2007; Bordoy and Burlando, 2013a). Using a time-splitting procedure the methodology was shown to improve substantially climate projections both in the period where the parameters were estimated and in a validation period, demonstrating that parameters were relatively insensitive to the calibration data set and therefore suitable for correcting future simulations (Bordoy and Burlando, 2013a).

Factors of change for several precipitation and air temperature statistics and different aggregation periods derived from bias corrected climate simulations were use to re-parametrize the multisite Neyman-Scott Rectangular Pulses and the multivariate Markovian models (Bordoy, 2013; Bordoy and Burlando, 2013b). Scaling properties of precipitation were used to extend climate precipitation statistics from daily to hourly time scale (Bordoy, 2013; Bordoy and Burlando, 2013b). Decades from 2011–2020 up to 2041–2050 were assumed each as a stationary period and therefore a different set of parameters (for each decade) was estimated and used in the generation of meteorological time series. The stochastic nature of the precipitation and temperature generators allows us to simulate multiple possible trajectories of future climate that account for natural climatic variability superposed on the climate change signal. Specifically, an ensemble size of 60 simulations was used in this study as a representative number which demonstrates the range of variability without excessively large computational requirements for the distributed hydrological model. Daily cloud transmissivity for the future climate was assumed to preserve the same statistical properties of the present and for each day of the year was randomly sampled from its empirical distribution constructed with the observed climate.

An ensemble of 60 simulations inclusive of precipitation and air temperature time series was also generated for the control scenario period 1991–2010 with the multisite Neyman-Scott Rectangular Pulses and the multivariate Markovian models. This climate ensemble allows to also take into account the climate stochasticity of the control scenario and most importantly to compare present and future hydrological simulations forced with consistently climate generated data.

Since for the simulations of present and future climate we did not produce gridded precipitation, we directly used the precipitation time series simulated at the stations with the stochastic precipitation generator. However, in order to preserve a realistic spatial distribution of precipitation, a correction factor (seasonally dependent) was applied to each grid cell. The correction factor represents the ratio between the climatological precipitation in a given cell and the climatological precipitation in the cell containing the station that is used as precipitation forcing for that given cell.

3 Results

3.1 Present climate confirmation

The performance of Topkapi-ETH in simulating hydrological dynamics was tested using discharge observations at 15 streamgauges in the Rhone catchment for the period 1990–2008 and snow-cover maps obtained as elaboration of the Moderate Resolution Imaging Spectroradiometer (MODIS) product MOD10A2 for the period 2000–2008 (Dedieu et al., 2010). Although only partially representative of catchment hydrological processes, this was the only available information to provide a distributed confirmation of model performance. Given the strong anthropogenic disturbances of the river flow, the capability of the model to simulate natural hydrological dynamics, river diversions, and reservoir operations cannot be separated at this stage. A full natural discharge can be assumed only for five of the most upstream stations, Rhone at Gletsch, Massa at Blatten bei Naters, Goneri at Oberwald, Lonza at Blatten, and Saltina at Brig.

Confirmation metrics in terms of determination coefficient (R^2), Nash-Sutcliffe efficiency (NS) and Root Mean Square Error (RMSE) for hourly, daily, monthly, and annual discharge in the period October 1990 through December 2008 were considered very satisfactorily (Table 1). Values of R^2 for daily discharge ranges from above 0.85 in the smaller upstream catchments to 0.7–0.8 for stations in the main reach of Rhone, down to 0.6–0.7 in the most disturbed catchments such as Vispa at Visp or Drance at Martigny. The only exceptions are represented by the station of Drance de Bagnes at Le Chable and Sionne at Sion for which the performance is significantly lower. The first station is highly affected by river diversions, which reduce significantly (about 70 %) the incoming discharge, relatively small errors in the representation of these structures can affect significantly the performance. The difference in the Sionne (for which we had only one and a half year of observations) are likely related to a wrong estimate of irrigation withdrawals that are significant in this area, or to river regulations that were not included in the model.

Computing the confirmation metrics at the hourly time scale did not decrease dramatically the performance of the model (Table 1). Despite the fact that reservoir operations cannot be exactly reproduced at this time scale, R^2 are generally only 0.05–0.10 lower than those computed at the daily aggregation scale for stations strongly affected by anthropogenic disturbances and almost identical for the other stations. Given the assumptions in the representation of anthropogenic disturbances, the model cannot simulate the exact operations at a given hour or day. However, we checked that the overall effect of human influence is accounted for realistically by looking at the oscillation of discharge in the winter period in stations downstream of major reservoirs. The amplitude of these oscillations is similar between the simulated and observed time series (not shown). The major differences between simulations and observation are in the summer peak discharge that are typically over-estimated in the simulations (not shown).

Determination coefficients and NS are highly satisfactory also for discharge aggregated at the monthly and annual scale, and RMSE are considerably smaller for these temporal aggregations (Table 1). While this result was expected at the monthly scale given the strong seasonality of discharge in most of the stations, the performance at the annual time scale is important because it demonstrates that we were able to reproduce well the discharge interannual variability for a 18 yr period.

The simulated and observed mean discharge are also very similar in all the examined stations (Table 1). This further supports the plausibility of the hydrological simulations, since it is very unlikely that parameter adjustments would lead to simulate correctly the total amount of streamflow in 15 stations representative of different catchment sizes, hydrological behaviors (glacial, snow, snow-pluvial regimes) and heavily influenced by human operations.

Simulated time series of basin areal fraction covered by snow and the temporally averaged spatial map of snow permanence were compared with the MODIS product MOD10A2 (Fig. 3). Comparison at the entire catchment scale is considered to be more robust than a pixel to pixel comparison given the high uncertainties associated with the MODIS product in complex topographic regions and its 8 day time scale. The comparison is satisfactory since model simulations and MODIS product agree on the dynamics of snow-cover of the upper Rhone catchment including the residual 15 % snow cover in summer. Only a small delay in snow melting in model simulation is detected (Fig. 3). This delay can also be explained with the problem of MODIS in classifying patchy snow at the end of the melting season or persistent snow cover below vegetation. The spatial distributions of snow cover are also matching well with small over-prediction of snow cover time for intermediate elevations.

Results for irrigation and domestic/industrial water consumption cannot be tested given the absence of multi-annual estimates of these quantities. However, from the model simulation, they appear to influence the overall hydrological budget of the upper Rhone in a negligible way, at least at the basin scale. We cannot exclude that withdrawals for irrigation can have important local effects but these cannot be tested due to the lack of more specific information.

3.2 Natural discharge confirmation

A great opportunity offered by the Rhone case study is the availability of high-quality streamflow time series extending back to the beginning of the 20th century. Specifically, in six stations observations of discharge were available for several (15–45) years before the construction of the reservoirs and diversion network (i.e. before 1950). Observations for this "pre-dam" period were compared with simulation in "natural-like" conditions, i.e. removing all the anthropogenic influence in the catchment. The comparison is presented in terms of discharge seasonality, averaging the discharge for each day of the year and representing also the observed and simulated discharge in the 1990–2008 period that includes anthropogenic influences (Fig. 4). The possible differences in climate forcing and glacier conditions between the "pre-dam" and the 1990–2008 period preclude a thorough confirmation of model results. Nonetheless these results represent a significant source of information to evaluate model performance in reproducing natural hydrological behavior and most important to effectively simulate the anthropogenic disturbances.

Results confirm that the model simulations are capable to reproduce the effect of human operations on discharge extremely well (Fig. 4). The reservoir storage of water during the summer period and the successive release in winter months is evident at the stations of the main reach of Rhone (Rhone at Port du Scex, Rhone at Sion, and Rhone at Branson). At the stations of Vispa at Visp and Drance de Bagnes at La Chable the significant fraction of discharge that is diverted outside these catchments is evident, although for Vispa at Visp the simulated alteration during summer is partially underestimated. Some difference between simulated and observed discharge can be noticed for the station of Grande Eau at Aigle where there is a positive bias in the simulated discharge during the spring season, most probably due to an overestimation of the winter precipitation in this area of the catchment. A tendency of the simulated natural

Title Page
Abstract | Introduction
Conclusions | References
Tables | Figures
◀| |▶
◀ ▶
Back | Close
Full Screen / Esc
Printer-friendly Version
Interactive Discussion

discharge to anticipate the observed “pre-dam” discharge in spring can be noticed at several stations. This is not surprising given the fact that the period before 1950 was colder than the 1990–2008 and therefore allowed a later onset of snow-melting.

3.3 Future climate projections

3.3.1 Changes in hydrological budget

Downscaling scenarios for different decades driven by different climate models show rather variable results for discharge at the basin scale mostly as a consequence of stochastic variability in precipitation (Table 2). The standard deviation of the stochastic ensemble in a 10 yr period (50–100 mm yr^{-1}) is comparable or larger than the projected change in discharge. Therefore assessments about changes in mean discharge over the entire upper Rhone basin remain very uncertain. The simulations directly driven by the GCM ECHAM5 averaged over the catchment and through the simulated stochastic ensembles predicted a decrease of about 100 mm yr^{-1} (or 10 % of the total annual discharge) for the middle of the 21st century. This is the result of an almost constant or slightly decreasing precipitation and of a warming of 0.9 °C when the 2040–2050 is compared with 1992–2010 (Table 2). The year 1991 is used as spin-up and excluded from the result analysis. For downscaling scenarios driven by the two RCMs, RegCM3 and REMO, the decrease is less than 50 mm yr^{-1} or < 5 %, and an increase is projected for intermediate decades 2011–2030 (Table 2). In fact, simulations driven by stochastic downscaling using the RCMs realizations predict an increase of precipitation of about 50–250 mm yr^{-1} for the period 2011–2040 and a less marked increase (70–120 mm yr^{-1}) afterwards (2041–50) with respect to the 1992–2010 control period (Table 2). The simulated warming is rather similar across all of the downscaling scenarios.

The other major components of the hydrological budget, i.e. evapotranspiration and ice melt are also shown in Table 2. Evapotranspiration remains almost constant for all of the scenarios up to the decade 2021–2030 and tend to slightly increase in the RCM driven scenarios (25–35 mm yr^{-1}) by the middle of the century as a result of a shorter period with snow-cover. Stochastic variability of evapotranspiration in a 10 yr period is in the order of 8–10 mm yr^{-1}, a quantity smaller than the projected change for the 2041–2050 decade. Average changes in ice melt are very similar regardless of the climate models used to drive the stochastic downscaling. This is clear when the annual cycle of ice melt of the control scenario and 2041–2050 period are analyzed for the three forcing scenarios (Fig. 5). A reduction of about 100 mm yr^{-1} is predicted to occur already by the 2021–2030 period and to stabilize afterwards, reducing significantly the ice melt contribution to total annual runoff, from about 13 % to about 4 %. Changes in ice melt are considered robust since they are much larger than the stochastic variability expected in a 10 yr period, i.e. about 10 mm yr^{-1}. Ice melt experienced a strong reduction that takes place in the second part of the summer in August and September (Fig. 5). Glaciated area and volumes are projected to decrease by about 50 % by the year 2050, with most of the reduction already occurring within the year 2020. This leads to a complete disappearance of glaciers below 2500 m a.s.l. but to negligible consequences for glaciers above 3500 m a.s.l.

The basin average quantities in Table 2 are not able to capture the spatial variability of the projected changes. Therefore, we analyzed changes for the 15 sub-catchments upstream of the streamgauges separately (Fig. 6). Regardless of the driving climate model, the uncertainty in the projection is higher for the catchments with a large glacierized area such as Rhone at Gletsch, Massa at Blatten bei Naters, Goneri at Oberwald and tend to decrease strongly for stations that are influenced by reservoir operations and river diversions such as Drance de Bagnes at Le Chable, Drance at Martigny, and Vispa at Visp. Despite the very large uncertainties indicated by the box-plots a robust signal toward a decrease in discharge can be detected in the catchments that contains a large glacierized area (e.g. Rhone at Gletsch). Conversely, a robust signal toward an increase was detected in the catchments located in the north-west side of the Rhone (Sionne at Sion and Grande Eau at Aigle), where the predicted precipitation increase is larger. For stations located within the main Rhone river (Rhone at Reckingen, at Brig, at Sion, at Branson, and at Port du Scex), the sign of change in discharge is uncertain and the most plausible conclusion is a lack of change.

3.3.2 Changes in seasonality and elevation dependence

Changes across downscaling scenarios are more consistent for seasonality of runoff. The average monthly discharge for simulations in two different periods 1992–2010 and 2041–2050 is compared in Fig. 7. The uncertainty on seasonality due to different climate models and to stochasticity is high, as indicated by the overlaps during a large part of the year among the bands representing future and control scenarios. However, projections show an increase of runoff in the period April–May due to an earlier beginning of the snow melt season and, more importantly, due to a larger amount of deposited snow as a consequence of enhanced winter precipitation (Fig. 7). This pattern is clear in catchments of the western part of the upper Rhone basin that experience the strongest increase in precipitation (e.g. Grande Eau, Drance) and tend to be less remarkable elsewhere. Snow melt is expected to remain unchanged or to slightly increase at elevations below 3000 m a.s.l. as a consequence of larger winter precipitation (Fig. 8). A consistent result is an increase of snow melt of about 100–200 mm yr^{-1} at elevations above 3000 m a.s.l., due to the warmer climate (Fig. 8). Despite increased snow melt, runoff in summer period (July, August, and beginning of September) for the decade 2040–50 is significantly less (even fully accounting for uncertainty) than in the control scenario. This is appreciable in all of the stations (Fig. 7) with a decrease that can be quantified in about 25 % for the entire Rhone basin and up to 50 % for the highly glacierized catchments (e.g. Rhone at Gletsch, Vispa at Visp). For basins without glaciers the decrease is smaller or null.

Given the significance of ice melt contribution to the total runoff in the sub-catchment of Rhone located at the highest altitudes and its dampened importance downstream, changes in the average discharge were sorted according to the upstream catchment average elevation for 297 selected points distributed throughout the river network. Despite the uncertainties imposed by the stochastic ensembles and by the driving

GCM/RCM, the elevational dependence effect of climate change appears as a very robust feature (Fig. 9). Catchments with the highest average elevation are expected to experience the most significant decrease in mean discharge, while catchments with the lowest average elevation show a tendency toward a small increase. Such a result is a combination of three effects, (i) the strong correlation of glacierized area with elevation and therefore reduction in the ice melt contribution; (ii) a larger increase of evapotranspiration at higher elevation due to reduced ice cover and duration of snow cover; (iii) the increase in precipitation in the north-west portion of the Rhone catchment where the lowest elevation catchments are also located.

The elevation dependent effect of climate change is also clear when the spatial distribution of changes in average discharge $\mathrm{mm\,yr^{-1}}$ between 1992–2010 and 2041–2050 are shown for the stochastic downscaling driven by RegCM3 (Fig. 10a). We can notice the effect that the river network has in dampening the negative changes in runoff in the river reaches downstream glacerized area and the positive changes in river reaches in the area where precipitation increase is stronger. The net result is a negligible change of mean discharge in the main Rhone. Interplay of human infrastructure with climate change effect is also appreciable, especially in the south-west part of the upper Rhone basin. This interplay is rather complicated because it tends to both emphasize and reduce natural climate change effects.

3.3.3 Changes in hydrological extremes

Analyzing changes in mean discharge and seasonality is only one way to look at climate change effects. Changes in higher order statistics can be very important for many practical applications. Percentage changes in the annual maximum and minimum discharge between 1992–2010 and 2041–2050 for the 297 selected points are analyzed for three different aggregation times: 1 h, 1 day and 30 days (Fig. 11 for the stochastic downscaling driven by RegCM3). The uncertainty coming from the stochastic ensemble in predicting maximum discharge is rather large. However, for 1 h and 1 day aggregation time, an increase of peak discharge of about 15–25 % (larger for 1 h) represents the most probable prediction for many river sections. This result is confirmed by the scenarios driven with different climate models (not shown), making it largely independent on the predicted change in mean precipitation. Elevation effects cannot be detected. Changes in minimum discharge for all of the aggregation periods and in maximum 30 days discharge are dominated by uncertainty, and a lack of change is the most probable projection (Fig. 11). Only simulations driven by ECHAM5 show a tendency toward a reduction of minimum discharge for the three aggregation periods (not shown).

The spatial distribution of average changes between 1992–2010 and 2041–2050 in daily maximum and minimum discharge obtained using the stochastic downscaling driven by RegCM3 (Fig. 10b, c) shows that interaction between reservoirs/diversions and natural flow are at play and that the geographical distribution of precipitation is very important. There are several Rhone tributaries in the west and north-west parts of the catchment where peak discharge is expected to increase significantly (20–50 %). Increases of peak flow tend to be dampened in the main Rhone river, where the average projected increase is about 10–20 %. Changes in daily minimum discharge are typically very small (< 5 %), except in a few river reaches downstream reservoirs where larger decreases are simulated.

3.3.4 Changes in reservoir levels, irrigation and water consumption

Changes in the mean discharge and its seasonality are expected to affect also the storage of the reservoirs and thus the hydropower operations. Seasonality of simulated reservoir levels are compared for two periods 1992–2010 and 2041–2050 (Fig. 12 for the stochastic downscaling driven by RegCM3 but similar results are obtained with other driving climate models). Given the fact that the operational rules are assumed unchanged in the future, reservoir levels mostly follow the availability of water during spring and summer months. In the period 2041–2050, the levels are significantly lower than in the control scenario in summer and autumn for several reservoirs such as Cleuson, Mattmark, Grand Dixence, Moiry, Mauvoisin that rely on ice melted water. The differences are typically larger than the spread induced by stochastic variability.

Consistently among the different driving climate models and for the entire ensemble of stochastic simulations irrigation and water consumption for domestic/industrial uses are predicted to be well satisfied in all the examined future decades and to be comparable with the control scenario (not shown). This is the results of the relatively small impact of these quantities in the overall water budget of the upper Rhone basin.

4 Discussion

We provided for the first time a quantification of present day anthropogenic disturbances in the hydrological budget of the upper Rhone basin. A series of infrastructures and operations that are affecting the natural hydrological regime, such as river diversions, reservoirs, water withdrawals for domestic/industrial and irrigation uses were implemented in a distributed hydrological model. We included these components at a level of detail rarely used for watersheds of this size (> 5000 km^2) and hydrological modeling of this complexity. Despite the fact that part of the available information was far from ideal, a comparison between (i) simulated and observed flows in the period 1990–2008 and (ii) seasonality of simulated natural flows and observations for the pre-dam period gave highly satisfactory results and supported the assumptions (Fig. 4). We acknowledge that the quality of the RhiresD gridded precipitation product combined with a knowledge of the water infrastructure configuration contributed significantly to the overall model performance across the entire basin, highlighting once more the paramount importance of boundary conditions in hydrological modeling.

For several subcatchments (e.g. Drance and Vispa catchments), climate induced changes on the hydrological budget (Fig. 7) are expected to be significantly smaller than changes occurred after the construction of the hydraulic infrastructure during the 50's and 60's. Our results demonstrate that heavily regulated catchments also have the property to significantly reduce the uncertainty in climate change hydrological predictions (Fig. 6). This is mostly related to the fact that flow in these catchments is controlled by river diversions and reservoirs that are assumed to operate similarly in the future and buffer the climate variability to a certain extent. New management rules or a significantly different energy demand might, however, reduce this effect. Conversely, the largest uncertainties were found for natural and highly glacierized catchments (e.g. Rhone at Gletsch, Massa at Blatten bei Naters). Uncertainties and stochastic variability in future air temperature but mostly in changes of precipitation regime lead to a large scatter in the projections. More in general, the interplay between infrastructure and climate change is rather complex and depends on local situations, for instance on the ratio between predicted natural discharge and diverted flow.

Climate change impacts were found to be elevation dependent regardless of the climate model driving the stochastic downscaling. This is connected to the loss of glacier area and reduction of ice melted water that is consistent among the downscaled scenarios driven by the different climate models (Fig. 5). Noticeably, we do not need a further warming for depleting most of the existing glacier resources that are not renewable even with the 1992–2010 climate as a forcing. Uncertainty related to the simplified method used to initialize the glacier thickness in the entire upper Rhone basin cannot be directly evaluated and are probably responsible for a rather abrupt decrease of the ice melt contribution. However, the fact that interannual variability of discharge was well simulated for a historical period of 18 yr supports the assumptions on initialization of ice cover and thickness at the spatial scale of the hydrological simulations. Ice melt reduction has a signal far larger than stochastic variability (Table 2) and is dictated by the disappearance of low elevation glaciers that were mostly contributing to streamflow in August and September (Fig. 5). Low elevation glaciers were snow-free during this period and contributed significantly (about 30–40 %) to the total basin runoff. These estimates are comparable to the results of Huss (2011) who used a very different methodology. The amount of snow melt is projected to remain the same or rather increase when 1992–2010 is compared with later decades (Fig. 8). This result is rather consistent among the downscaled scenarios and is related to the fact that precipitation in February to April is predicted to increase and snow-melt contribution from elevations above 3200 m a.s.l. is also increasing as a consequence of warmer temperatures.

The overall climate change effect on streamflow is thus strongly dependent on the amount of glacierized areas of a catchment. Changes in precipitation are rather uncertain since they are variable across decades and typically the signal is below the noise induced by stochastic climate variability (Table 2). Uncertain changes in total precipitation combined with a significant decrease of ice melt imply a considerable reduction of average runoff for high elevation catchments fed by glacier sources. This reduction is progressively dampened downstream at lower elevations. The total upper Rhone average streamflow is indeed similar or just slightly smaller when future decades are compared with the period 1992–2010. However, a change in seasonality with larger April-May flows and most importantly lower August–September flows tends to emerge out of the interannual variability. The role of evapotranspiration change was found to be less important in such a mountainous environment. For this reason, we expect that the simple methodology used in Topkapi-ETH for calculating evapotranspiration is not affecting significantly the overall result of the analysis.

There is a robust signal independent of the GCM/RCM used to drive the downscaling of an increase of maximum hourly (+25 %) and daily discharge (+10–20 %) across almost the entire basin. This signal is strong despite the interannual variability of precipitation, i.e. there are very few stochastic trajectories where maximum discharge is projected to decrease (Fig. 11). Such a result might have non-negligible implication for flood risk management in the upper Rhone. A shift in the seasonality of flood occurrence was very difficult to detect due to the fact that both spring-summer melting and early autumn storm (the flood prone season in the area) may lead to the largest flood peak in a given year. Note that these results are obtained without including specific reservoir operations that can be undertaken to reduce the peak flow during the flood event (Jordan, 2007; Jordan et al., 2012) and that are likely to offer a possibility to partially regulate these expected increase in streamflow maxima.

Hydropower production in the upper Rhone is likely to be significantly affected in the near future. Despite the overall uncertain in projections, reservoirs that are fed with a significant fraction of water coming from glacierized catchments will not be able to maintain the same water levels in the late summer and autumn if management operations are not changed (Fig. 12). Lower reservoir levels have straightforward implications for hydropower production because of less available water to turbine and a lower hydraulic head. We argue that even with a different management of the dams, the total energy production of the control scenario would be unlikely maintained in the 2030–2050 period, simply because hydropower companies are at present using water from ice melt that is not a renewable resource even with the current climate. This result supports previously published research (Schaefli et al., 2007; Finger et al., 2012) and emphasizes its relevance at the catchment scale. Implications are more evident for the reservoirs of Mattmark, Grand Dixence, Mauvoisin, and Cleuson. Note that reservoirs (e.g. Tseuzier) fed by rainwater or snow-melt are not affected by such an effect.

These results lead us to argue that broad impacts of climate change in water resources of the entire Alpine areas might have been overestimated in the past. The available water resources in the main valley and the water export from the basin (the water tower) are much less affected than small mountainous glacierized basins. Most previous studies focusing only on high-elevation catchments have provided a partial vision of hydrological change in the Alps (Zierl and Bugmann, 2005; Horton et al., 2006; Schaefli et al., 2007; Rössler et al., 2012; Uhlmann et al., 2012; Finger et al., 2012; Farinotti et al., 2012). Simulated hydrological changes are significantly dampened at lower elevations and with increasing area, with the exception of a reduction of late summer flows that propagate throughout the entire upper Rhone basin. Nonetheless, we acknowledge that changes in high elevation catchments can have a paramount importance because these streams are supporting biodiversity of aquatic environments (Brown et al., 2007; Milner et al., 2009; Jacobsen et al., 2012), as well as are intensively utilized for hydropower production.

5 Conclusions

A distributed long-term hydrological balance of the upper Rhone basin was provided including forcing due to climate change and anthropogenic disturbances simulated at an unprecedent level of detail for catchment of this size and complexity. Model performance in reproducing present-day and natural flow regimes were highly satisfactory and result from the preservation of relatively high-resolution topography, the quality of the precipitation input, and a thorough implementation of boundary conditions. A catchment integrated and distributed approach accounting for strong anthropogenic disturbances was found very important for an overall analysis of climate change effects on the hydrological cycle at the scale of interest for water management. We demonstrated that in the upper Rhone catchment a large environmental change experiment took place about sixty years ago with the construction of the existing hydraulic infrastructure, which likely affected, in several reaches, streamflow regime more than the climate change signal expected by the middle of the 21st century. We found an elevational dependence of climate change impacts with a larger threat for high-elevation streams than for main rivers in the valleys. Ice melt contribution was identified as a crucial process for future predictions of streamflow and its reduction appears unavoidable even without any additional climate warming. Consequences for aquatic biodiversity and hydropower production are possibly very significant. At the entire catchment scale a reduction of summer discharge and an increase of maximum flows appear to be the most significant changes.

Acknowledgements. The present study is part of the ACQWA Project (Assessing Climate impacts on the Quantity and quality of WAter), funded within the seventh Framework Program of the European Union, contract 212250, www.acqwa.ch. We thank Jean-Pierre Dedieu for elaborating snow cover maps from the MODIS product within the ACQWA project, and Juerg Fuhrer and Pascalle Smith for making available the soil map of the upper Rhone. Meteorological data were provided by MeteoSwiss, the Federal Office of Meteorology and Climatology. We finally thank people from Kraftwerke Mattmak, Compagnia Valdostana delle Acque (CVA), and Officine Idroelettriche della Maggia (OFIMA) for providing data about reservoir characteristics, levels and discharge.

References

Anandhi, A., Frei, A., Pierson, D. C., Schneiderman, E. M., Zion, M. S., Lounsbury, D., and Matonse, A. H.: Examination of change factor methodologies for climate change impact assessment, Water Resour. Res., 47, W03501, doi:10.1029/2010WR009104, 2011. 3757

Bahr, D. B., Meier, M. F., and Peckham, S. D.: The physical basis of glacier volume-area scaling, J. Geophys. Res., 102, 20355–20362, 1997. 3753

Bauder, A., Funk, M., and Huss, M.: Ice-volume changes of selected glaciers in the Swiss Alps since the end of the 19th century, Ann. Glaciol., 46, 145–149, doi:10.3189/172756407782871701, 2007. 3753

Beniston, M.: Mountain weather and climate: a general overview and a focus on climatic change in the alps, Hydrobiologia, 562, 3–16, doi:10.1007/s10750-005-1802-0, 2006. 3745

Beniston, M.: Impacts of climatic change on water and associated economic activities in the Swiss Alps, J. Hydrol., 412–413, 291–296, 2012. 3745

Beniston, M., Stoffel, M., and Hill, M.: Impacts of climatic change on water and natural hazards in the Alps: can current water governance cope with future challenges? Examples from the European “ACQWA” project, Environ. Sci. Policy, 14, 734–743, doi:10.1016/j.envsci.2010.12.009, 2011. 3745

Bordoy, R.: Spatiotemporal downscaling of climate scenarios in regions of complex orography, Ph.D. thesis, ETH Zurich, Switzerland, 2013. 3748, 3757, 3758

Bordoy, R. and Burlando, P.: Bias correction of regional climate model simulations in a region of complex orography, J. Appl. Meteorol. Clim., 52, 82–101, doi:10.1175/JAMC-D-11-0149.1, 2013a. 3758

Bordoy, R. and Burlando, P.: Stochastic downscaling of precipitation to high-resolution scenarios in orographically complex regions. Part 2: Downscaling methodology, Water Resour. Res., submitted, 2013b. 3757, 3758

Bordoy, R. and Burlando, P.: Stochastic downscaling of precipitation to high-resolution scenarios in orographically complex regions. Part 1: Model evaluation, Water Resour. Res., submitted, 2013c. 3748

Brown, L. E., Hannah, D. M., and Milner, A. M.: Vulnerability of alpine stream biodiversity to shrinking glaciers and snowpacks, Glob. Change Biol., 13, 958–966, 2007. 3771

Brutsaert, W.: Hydrology, An Introduction, Cambridge University Press, Cambridge, UK, 2005. 3749

Burlando, P. and Rosso, R.: Extreme storm rainfall and climatic change, Atmos. Res., 27, 169–189, 1991. 3757

Burlando, P. and Rosso, R.: Effects of transient climate change on basin hydrology. 1. Precipitation scenarios for the Arno river, central Italy, Hydrolog. Proc., 16, 1151–1175, 2002. 3757

Burton, A., Kilsby, C. G., Fowler, H. J., Cowpertwait, P. S. P., and O'Connell, P.: RainSim: a spatial-temporal stochastic rainfall modelling system, Environ. Modell. Softw., 23, 1356–1369, doi:10.1016/j.envsoft.2008.04.003, 2008. 3757

Burton, A., Fowler, H. J., Blenkinsop, S., and Kilsby, C. G.: Downscaling transient climate change using a Neyman-Scott rectangular pulses stochastic rainfall model, J. Hydrol., 381, 18–32, doi:10.1016/j.jhydrol.2009.10.031, 2010. 3748, 3757

Camporese, M., Paniconi, C., Putti, M., and Orlandini, S.: Surface-subsurface flow modeling with path-based runoff routing, boundary condition-based coupling, and assimilation of multisource observation data, Water Resour. Res., 46, W02512, doi:10.1029/2008WR007536, 2010. 3750

Carenzo, M., Pellicciotti, F., Rimkus, S., and Burlando, P.: Assessing the transferability and robustness of an enhanced temperature-index glacier melt model, J. Glaciol., 55, 258–274, 2009. 3750

Christensen, J. H., Kjellström, E., Giorgi, F., Lenderink, G., and Rummukainen, M.: Weight assignment in regional climate models, Clim. Res., 44, 179–194, doi:10.3354/cr00916, 2010. 3748

Ciarapica, L. and Todini, E.: TOPKAPI: a model for the representation of the rainfall-runoff process at different scales, Hydrolog. Proc., 16, 207–229, 2002. 3747, 3749

Corripio, J.: Vectorial algebra algorithms for calculating terrain parameters from DEMs and solar radiation modelling in mountainous terrain, Int. J. Geogr. Inform. Sci., 17, 1–23, 2003. 3749

Dedieu, J.-P., Boos, A., Kiage, W., and Pellegrini, M.: Snow cover retrieval over Rhone and Po river basins from MODIS optical satellite data (2000–2009), Geophys. Res. Abstr., EGU2010-5532, EGU General Assembly 2010, Vienna, Austria, 2010. 3759

Déqué, M., Jones, R. G., Wild, M., Giorgi, F., Christensen, J. H., Hassell, D. C., Vidale, P. L., Rockel, B., Jacob, D., Kjellström, E., deCastro, M., Kucharski, F., and van den Hurk, B.: Global high resolution versus Limited Area Model climate change projections over Europe: quantifying confidence level from PRUDENCE results, Clim. Dynam., 25, 653–670, doi:10.1007/s00382-005-0052-1, 2005. 3748

Deser, C., Phillips, A., Bourdette, V., and Teng, H.: Uncertainty in climate change projections: the role of internal variability, Clim. Dynam., 38, 527–546, doi:10.1007/s00382-010-0977-x, 2012. 3748

Dobler, C., Hagemann, S., Wilby, R. L., and Stötter, J.: Quantifying different sources of uncertainty in hydrological projections in an Alpine watershed, Hydrol. Earth Syst. Sci., 16, 4343–4360, doi:10.5194/hess-16-4343-2012, 2012. 3745

Ebel, B. A., Loague, K., Montgomery, D. R., and Dietrich, W. E.: Physics-based continuous simulation of long-term near-surface hydrologic response for the Coos Bay experimental catchment, Water Resour. Res., 44, W07417, doi:10.1029/2007WR006442, 2008. 3750

Elsasser, H. and Bürki, R.: Climate change as a threat to tourism in the Alps, Clim. Res., 20, 253–257, 2002. 3745

Farinotti, D., Huss, M., Bauder, A., and Funk, M.: An estimate of the glacier ice volume in the Swiss Alps, Global Planet. Change, 68, 225–231, 2009a. 3753

Farinotti, D., Huss, M., Bauder, A., Funk, M., and Truffer, M.: A method to estimate the ice volume and ice-thickness distribution of alpine glaciers, J. Glaciol., 55, 422–430, 2009b. 3753

Farinotti, D., Usselmann, S., Huss, M., Bauder, A., and Funk, M.: Runoff evolution in the Swiss Alps: projections for selected high-alpine catchments based on ENSEMBLES scenarios, Hydrolog. Proc., 26, 1909–1924, doi:10.1002/hyp.8276, 2012. 3746, 3771

Fatichi, S., Ivanov, V. Y., and Caporali, E.: Simulation of future climate scenarios with a weather generator, Adv. Water Resour., 34, 448–467, doi:10.1016/j.advwatres.2010.12.013, 2011. 3752, 3757

Fatichi, S., Ivanov, V. Y., and Caporali, E.: A mechanistic ecohydrological model to investigate complex interactions in cold and warm water-controlled environments. 1 Theoretical framework and plot-scale analysis, J. Adv. Model. Earth Syst., 4, M05002, doi:10.1029/2011MS000086, 2012a. 3750

Fatichi, S., Ivanov, V. Y., and Caporali, E.: A mechanistic ecohydrological model to investigate complex interactions in cold and warm water-controlled environments. 2. Spatiotemporal analyses, J. Adv. Model. Earth Syst., 4, M05003, doi:10.1029/2011MS000087, 2012b. 3750, 3756

Fatichi, S., Ivanov, V. Y., and Caporali, E.: Assessment of a stochastic downscaling methodology in generating an ensemble of hourly future climate time series, Clim. Dynam., online first, doi:10.1007/s00382-012-1627-2, 2013. 3748, 3749

Finger, D., Heinrich, G., Gobiet, A., and Bauder, A.: Projections of future water resources and their uncertainty in a glacierized catchment in the Swiss Alps and the subsequent effects on hydropower production during the 21st century, Water Resour. Res., 48, W02521, doi:10.1029/2011WR010733, 2012. 3746, 3747, 3771

Fuhrer, J., Beniston, M., Fischlin, A., Frei, C., Goyette, S., Jasper, K., and Pfister, C.: Climate risks and their impact on agriculture and forests in Switzerland, Climatic Change, 79, 79–102, doi:10.1007/s10584-006-9106-6, 2006. 3745

Hawking, E. and Sutton, R.: The potential to narrow uncertainty in regional climate predictions, B. Am. Meteorol. Soc., 90, 1095–1107, doi:10.1175/2009BAMS2607.1, 2009. 3748

Hawking, E. and Sutton, R.: The potential to narrow uncertainty in projections of regional precipitation change, Clim. Dynam., 37, 407–418, doi:10.1007/s00382-010-0810-6, 2011. 3748

Hill, M., Wallner, A. and Furtado, J.: Reducing vulnerability to climate change in the Swiss Alps: a study of adaptive planning, Clim. Policy, 10, 70–86, doi:10.3763/cpol.2008.0536, 2010. 3745

Horton, P., Schaefli, B., Mezghani, A., Hingray, B., and Musy, A.: Assessment of climate-change impacts on alpine discharge regimes with climate model uncertainty, Hydrol. Process., 20, 2091–2109, 2006. 3746, 3771

Huss, M.: Present and future contribution of glacier storage change to runoff from macroscale drainage basins in Europe, Water Resour. Res., 47, W07511, doi:10.1029/2010WR010299, 2011. 3745, 3769

IPCC: Special Report on Emissions Scenarios. A Special Report of Working Group III of the Intergovernmental Panel on Climate Change, Cambridge University Press, Cambridge, UK and New York, NY, USA, 2000. 3748

Ivanov, V. Y., Vivoni, E. R., Bras, R. L., and Entekhabi, D.: Preserving high-resolution surface and rainfall data in operational-scale basin hydrology: a fully-distributed physically-based approach, J. Hydrol., 298, 80–111, doi:10.1016/j.jhydrol.2004.03.041, 2004. 3750

Ivanov, V. Y., Bras, R. L., and Vivoni, E. R.: Vegetation-hydrology dynamics in complex terrain of semiarid areas: 1. A mechanistic approach to modeling dynamic feedbacks, Water Resour. Res., 44, W03429, doi:10.1029/2006WR005588, 2008. 3750

Jacob, D., Bärring, L., Bøssing Christensen, O., Hesselbjerg Christensen, J., de Castro, M., Déqué, M., Giorgi, F., Hagemann, S., Hirschi, M., Jones, R., Kjellström, E., Lenderink, G., Rockel, B., Sánchez, E., Schär, C., Seneviratne, S. I., Somot, S., van Ulden, A., and van den Hurk, B.: An inter-comparison of regional climate models for Europe: model performance in present-day climate, Climatic Change, 81, 31–52, doi:10.1007/s10584-006-9213-4, 2007. 3758

Jacobsen, D., Milner, A. M., Brown, L. E., and Dangles, O.: Biodiversity under threat in glacier-fed river systems, Nature Climate Change, 2, 361–364, doi:10.1038/NCLIMATE1435, 2012. 3771

Jordan, F.: Modèle de prévision et de gestion des crues optimisation des opérations des aménagements hydroélectriques à accumulation pour la réduction des débits de crue, Ph.D. thesis, Ecole Polytechnique Fédérale de Lausanne, Lausanne, Switzerland, 2007. 3753, 3770

Jordan, F. M., Boillat, J.-L., and Schleiss, A. J.: Optimization of the flood protection effect of a hydropower multi-reservoir system, International Journal of River Basin Management, 10, 65–72, doi:10.1080/15715124.2011.650868, 2012. 3770

Knutti, R.: Should we believe model predictions of future climate change?, Philos. T. Roy. Soc. A, 366, 4647–4664, doi:10.1098/rsta.2008.0169, 2008. 3748

Koenig, U. and Abegg, B.: Impacts of climate change on winter tourism in the Swiss alps, J. Sustain. Tour., 5, 46–58, 1997. 3745

Kollet, S. J. and Maxwell, R. M.: Integrated surface-groundwater flow modeling: a free-surface overland flow boundary condition in a parallel groundwater flow model, Adv. Water Resour., 29, 945–958, 2006. 3750

Leander, R. and Buishand, T. A.: Resampling of regional climate model output for the simulation of extreme river flows, J. Hydrol., 332, 487–496, doi:10.1016/j.jhydrol.2006.08.006, 2007. 3758

Liu, Z. and Todini, E.: Towards a comprehensive physically-based rainfall-runoff model, Hydrol. Earth Syst. Sci., 6, 859–881, doi:10.5194/hess-6-859-2002, 2002. 3747, 3749

Liu, Z. and Todini, E.: Assessing the TOPKAPI non-linear reservoir cascade approximation by means of a characteristic lines solution, Hydrolog. Process., 19, 1983–2006, doi:10.1002/hyp.5662, 2005. 3749

Loizeau, J.-L. and Dominik, J.: Evolution of the Upper Rhone River discharge and suspended sediment load during the last 80 year and some implications for Lake Geneva, Aquat. Sci., 62, 54–67, 2000. 3754

Meile, T., Boillat, J. L., and Schleiss, A.: Hydropeaking indicators for characterization of the Upper-Rhone river in Switzerland, Aquat. Sci., 73, 171–182, doi:10.1007/s00027-010-0154-7, 2011. 3747

Milano, V.: Acquedotti, Hoepli, Milano, Italy, 1996. 3756

Milner, A. M., Brown, L. E., and Hannah, D. M.: Hydroecological response of river systems to shrinking glaciers, Hydrol. Process., 23, 62–67, doi:10.1002/hyp.7197, 2009. 3771

Pal, J. S., Giorgi, F., Bi, X., Elguindi, N., Solomon, F., Gao, X., Rauscher, S. A., Francisco, R., Zakey, A., Winter, J., Ashfaq, M., Syed, S. F., Bell, J. L., Diffenbaugh, N. S., Karmacharya, J., Konare, A., Martinez, D., daRocha, R. P., Sloan, L. C., and Steiner, A. L.: Regional climate modeling for the developing world: the ICTP regCM3 and regCNET, B. Am. Meteorol. Soc., 88, 1395–1409, doi:10.1175/BAMS-88-9-1395, 2007. 3758

Pellicciotti, F., Brock, B., Strasser, U., Burlando, P., Funk, M., and Corripio, J.: An enhanced temperature-index glacier melt model including the shortwave radiation balance: development and testing for Haut Glacier d'Arolla, Switzerland, J. Glaciol., 51, 573–587, 2005. 3750

Prein, A. F., Gobiet, A., and Truhetz, H.: Analysis of uncertainty in large scale climate change projections over Europe, Meteorol. Z., 20, 383–395, doi:10.1127/0941-2948/2011/0286, 2011. 3748

Priestley, C. and Taylor, R.: On the assessment of surface heat flux and evaporation using large-scale parameters, Mon. Weather Rev., 100, 81–92, doi:10.1175/1520-0493(1972)100<0081:OTAOSH>2.3.CO;2, 1972. 3749

Räisänen, J.: How reliable are climate models?, Tellus A, 59, 2–29, doi:10.1111/j.1600-0870.2006.00211.x, 2007. 3748

Rigon, R., Bertoldi, G., and Over, T. M.: GEOtop: A distributed hydrological model with coupled water and energy budgets, J. Hydrometeorol., 7, 371–388, 2006. 3750

Rixen, C., Teich, M., Lardelli, C., Gallati, D., Pohl, M., Pütz, M., and Bebi, P.: Winter tourism and climate change in the Alps: an assessment of resource consumption, snow reliability, and future snowmaking potential, Mt. Res. Dev., 31, 229–236, doi:10.1659/MRD-JOURNAL-D-10-00112.1, 2011. 3745

Roeckner, E., Bäuml, G., Bonaventura, L., Brokopf, R., Esch, M., Giorgetta, M., Hagemann, S., Kirchner, I., Kornblueh, L., Manzini, E., Rhodin, A., Schlese, U., Schulzweida, U., and Tompkins, A.: The atmospheric general circulation model ECHAM5. Part I: Model description, Tech. Rep. 349, Max Planck Institute for Meteorology, Hamburg, Germany, 2003. 3757

Rössler, O., Diekkrüger, B., and Löffler, J.: Potential drought stress in a Swiss mountain catchment – ensemble forecasting of high mountain soil moisture reveals a drastic decrease, despite major uncertainties, Water Resour. Res., 48, W04521, doi:10.1029/2011WR011188, 2012. 3746, 3771

Rosso, R.: Idrologia, The Real Book, CUSL, Milano, 2000. 3749

Schädler, B. and Weingartner, R.: Alpine Waters, Vol. 6, chap. Impact of climate change on water resources in the Alpine regions of Switzerland, 59–69, Springer-Verlag Berlin, Heidelberg, 2010. 3745

Schaefli, B., Hingray, B., and Musy, A.: Climate change and hydropower production in the Swiss Alps: quantification of potential impacts and related modelling uncertainties, Hydrol. Earth Syst. Sci., 11, 1191–1205, doi:10.5194/hess-11-1191-2007, 2007. 3746, 3771

Schwarb, M.: The Alpine precipitation climate evaluation of a high-resolution analysis scheme using comprehensive rain-gauge data, Ph.D. thesis, ETH Zurich, Switzerland, 2000. 3751

Shen, C. and Phanikumar, M. S.: A process-based, distributed hydrologic model based on a large-scale method for surface-subsurface coupling, Adv. Water Resour., 33, 1524–1541, doi:10.1016/j.advwatres.2010.09.002, 2010. 3750

Theurillat, J. P. and Guisan, A.: Potential impact of climate change on vegetation in the european alps: a review, Climatic Change, 50, 77–109, doi:10.1023/A:1010632015572, 2001. 3745

Uhlmann, B., Jordan, F., and Beniston, M.: Modelling runoff in a Swiss glacierized catchment – Part II: Daily discharge and glacier evolution in the Findelen basin in a progressively warmer climate, Int. J. Climatol., online first, doi:10.1002/joc.3516, 2012. 3746, 3771

Viviroli, D., Dürr, H. H., Messerli, B., Meybeck, M., and Weingartner, R.: Mountains of the world, water towers for humanity: typology, mapping, and global significance, Water Resour. Res., 43, W07447, doi:10.1029/2006WR005653, 2007. 3745

Viviroli, D., Archer, D. R., Buytaert, W., Fowler, H. J., Greenwood, G. B., Hamlet, A. F., Huang, Y., Koboltschnig, G., Litaor, M. I., López-Moreno, J. I., Lorentz, S., Schädler, B., Schreier, H., Schwaiger, K., Vuille, M., and Woods, R.: Climate change and mountain water resources: overview and recommendations for research, management and policy, Hydrol. Earth Syst. Sci., 15, 471–504, doi:10.5194/hess-15-471-2011, 2011. 3745

Wuest, M., Frei, C., Altenhoff, A., Hagen, M., Litschi, M., and Schar, C.: A gridded hourly precipitation dataset for switzerland using rain-gauge analysis and radar-based disaggregation, Int. J. Climatol., 30, 1764–1775, doi:10.1002/joc.2025, 2010. 3751

Zierl, B. and Bugmann, H.: Global change impacts on hydrological processes in Alpine catchments, Water Resour. Res., 41, W02028, doi:10.1029/2004WR003447, 2005. 3745, 3746, 3771

Table 1. Simulated (SIM.) and observed (OBS.) mean discharge [$m^3 s^{-1}$] and metrics of performance for the river sections corresponding to the 15 streamgauges in the observational period 1990–2008. R^2 is the coefficient of determination, RMSE is the root mean square error [$m^3 s^{-1}$] and NS is the Nash-Sutcliffe efficiency. Metrics of performance are evaluated for hourly, daily, monthly and annual aggregation periods except for Sionne–Sion where only one year and a half of observations was available.

	Mean Discharge		Hourly			Daily			Monthly			Annual		
Station	OBS. [$m^3 s^{-1}$]	SIM. [$m^3 s^{-1}$]	R^2	NS	RMSE	R^2	NS	RMSE	R^2	NS	RMSE	R^2	NS	RMSE
1 Rhone – Port du Scex	185.7	189.2	0.64	0.64	70.9	0.69	0.69	63.7	0.84	0.84	37.4	0.82	0.75	17.9
2 Rhone – Sion	104.2	111	0.75	0.75	45.9	0.81	0.8	40.2	0.91	0.91	23.3	0.9	0.8	10.3
3 Rhone – Branson	137.2	141.9	0.6	0.59	62.6	0.7	0.69	51.7	0.85	0.85	29.7	0.82	0.75	13.8
4 Drance – Martigny	10	12.2	0.61	0.57	5.9	0.67	0.62	5.3	0.78	0.7	3.9	0.86	0.33	2.36
5 Drance de Bagnes – Le Chable	2.06	2.18	0.36	0.22	1.6	0.43	0.33	1.4	0.54	0.41	1	0.69	0.65	0.29
6 Massa – Blatten bei Naters	14.3	14	0.88	0.87	7.2	0.89	0.89	6.5	0.95	0.95	3.9	0.8	0.78	1.6
7 Grande Eau – Aigle	4.68	4.59	0.63	0.59	2.2	0.68	0.67	1.9	0.82	0.82	1.23	0.79	0.74	0.46
8 Rhone – Gletsch	2.91	2.82	0.86	0.86	1.5	0.89	0.89	1.3	0.95	0.94	0.82	0.77	0.74	0.33
9 Lonza – Blatten	4.75	3.93	0.8	0.73	2.6	0.87	0.82	2.1	0.96	0.91	1.3	0.84	0.42	0.92
10 Vispa – Visp	17.1	19.3	0.46	0.45	15.3	0.64	0.6	12.3	0.82	0.73	8.3	0.67	0.52	3.3
11 Rhone – Reckingen	9.63	10.7	0.8	0.77	6.4	0.84	0.8	5.8	0.93	0.86	4.2	0.87	0.72	1.3
12 Goneri – Oberwald	2.43	2.38	0.71	0.71	1.7	0.77	0.77	1.5	0.89	0.88	0.95	0.81	0.79	0.25
13 Sionne – Sion	0.4	0.46	0.1	−0.07	0.48	0.08	-0.12	0.46						
14 Rhone – Brig	41.4	43.2	0.82	0.82	20.5	0.87	0.87	17.1	0.95	0.95	9.5	0.89	0.85	3.42
15 Saltina – Brig	2.26	2.31	0.67	0.67	1.7	0.76	0.76	1.4	0.83	0.81	0.87	0.87	0.86	0.2

Table 2. Values of simulated meteorological forcings and hydrological budget components for the control scenario 1992–2010 and for the four future decades using the stochastic downscaling simulations driven by ECHAM5, RegCM3, and REMO. The numbers refer to basin averaged quantities, Ta is the air temperature, Pr is the precipitation, ET is the evapotranspiration, Mg is the ice melt, and Q is the basin outlet discharge. The number after ± represents one standard deviation of the simulated values according to the stochastic ensembles.

Hydrological component	Ta [°C]	Pr [$\mathrm{mm\,yr^{-1}}$]	ET [$\mathrm{mm\,yr^{-1}}$]	Mg [$\mathrm{mm\,yr^{-1}}$]	Q [$\mathrm{mm\,yr^{-1}}$]
Control Scenario 1992–2010	1.92 ± 0.10	1265 ± 49	299 ± 6	141 ± 10	1046 ± 39
ECHAM5 2011–20	2.25 ± 0.11	1187 ± 85	291 ± 8	122 ± 15	981 ± 73
ECHAM5 2021–30	1.93 ± 0.13	1252 ± 78	300 ± 8	48 ± 9	945 ± 69
ECHAM5 2031–40	2.61 ± 0.12	1242 ± 63	312 ± 8	49 ± 11	938 ± 54
ECHAM5 2041–50	2.84 ± 0.14	1194 ± 90	301 ± 10	44 ± 10	911 ± 77
RegCM3 2011–20	2.14 ± 0.14	1388 ± 67	300 ± 10	111 ± 13	1154 ± 56
RegCM3 2021–30	1.91 ± 0.12	1546 ± 96	285 ± 9	38 ± 8	1201 ± 83
RegCM3 2031–40	2.53 ± 0.11	1408 ± 132	298 ± 9	44 ± 10	1106 ± 112
RegCM3 2041–50	2.77 ± 0.15	1331 ± 68	337 ± 8	41 ± 11	997 ± 55
REMO 2011–20	2.2 ± 0.13	1283 ± 118	293 ± 10	112 ± 14	1066 ± 99
REMO 2021–30	1.94 ± 0.12	1484 ± 100	294 ± 8	45 ± 10	1164 ± 88
REMO 2031–40	2.69 ± 0.11	1327 ± 106	326 ± 9	59 ± 11	1029 ± 95
REMO 2041–50	2.85 ± 0.12	1377 ± 88	326 ± 10	40 ± 7	1042 ± 76

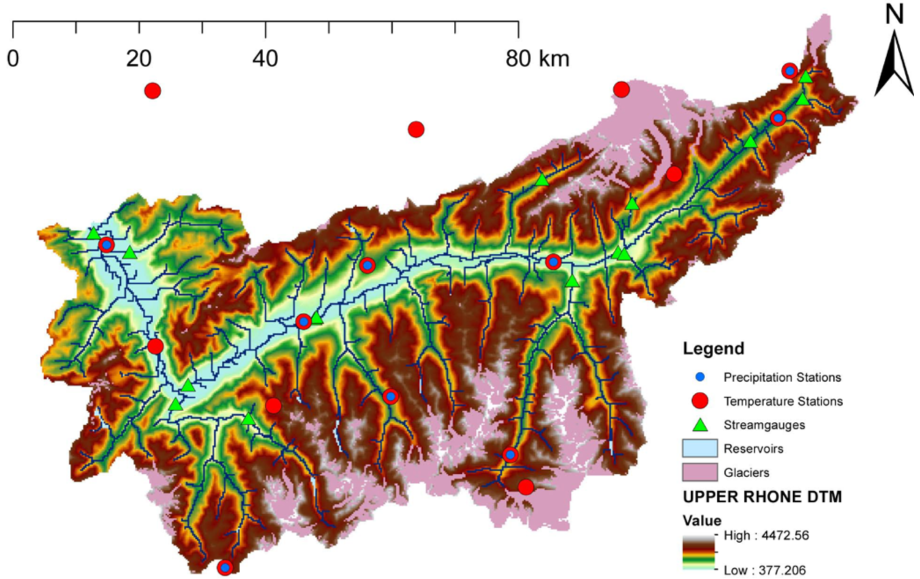

Fig. 1. A representation of Digital Terrain Model (DTM), glaciated areas, reservoirs, and monitoring network in the upper Rhone basin. The symbols indicate the locations of stations for measurement of precipitation (small blue circles), temperature (big red circles) and streamflow (green triangles).

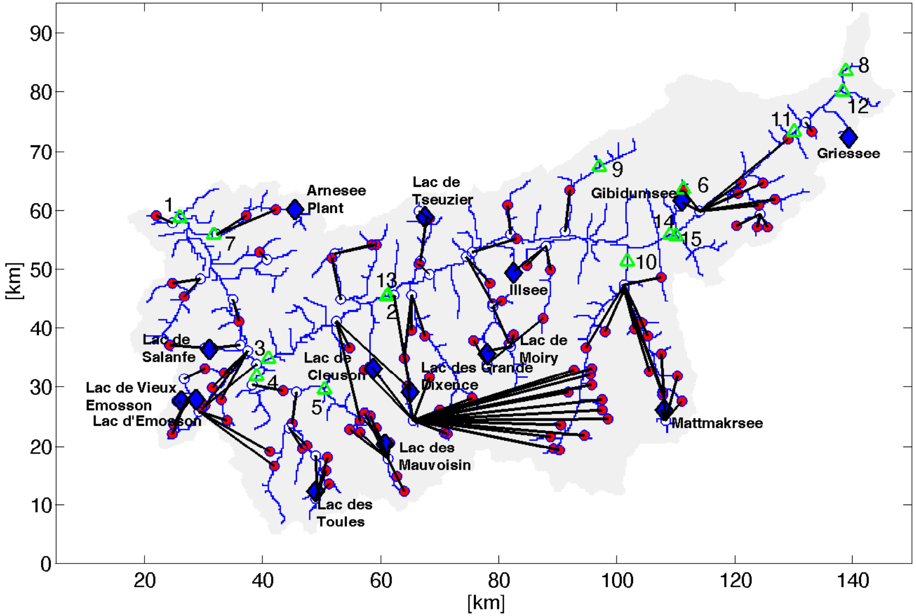

Fig. 2. A representation of the scheme of reservoirs and river diversions used in the hydrological modeling analysis. Reservoirs are represented with blue diamonds and with a given name, river diversions are represented with black lines, uptake points with red dots, return points with white dots. The 15 streamgauges are represented with green triangles and with an identifying number.

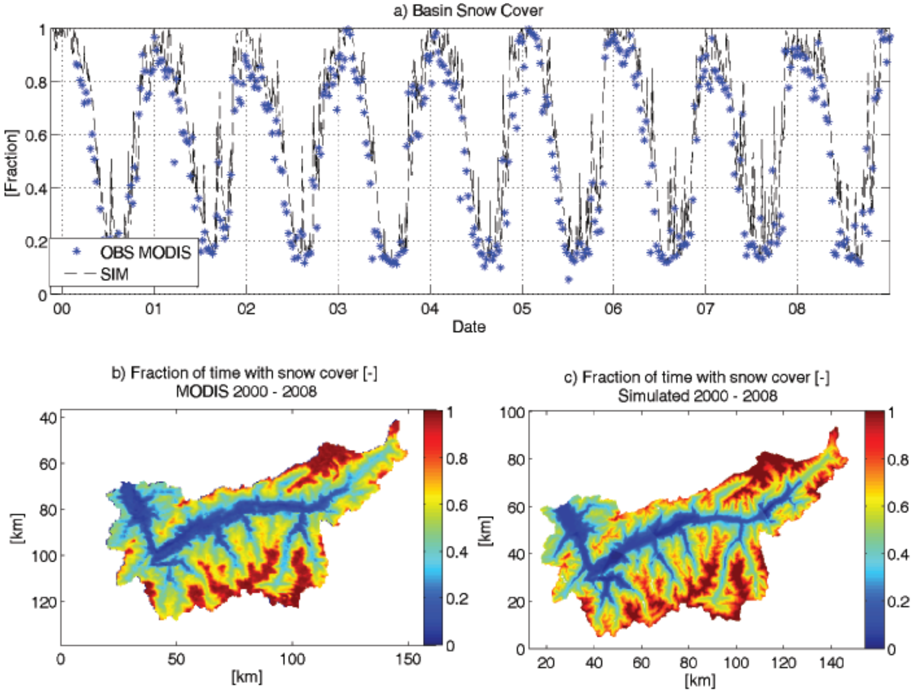

Fig. 3. The fraction of time with snow cover for the upper Rhone basin over the period of January 2000 through December 2008. **(a)** The time series of snow cover fraction spatially averaged across the entire basin from remote sensing estimates and simulation; **(b)** the spatial map of snow cover from MODIS product MOD10A2, temporally averaged over the 2000–2008 period; **(c)** the spatial map of snow cover (assumed as snow water equivalent larger than 10 mm) from simulations, temporally averaged over the 2000–2008 period.

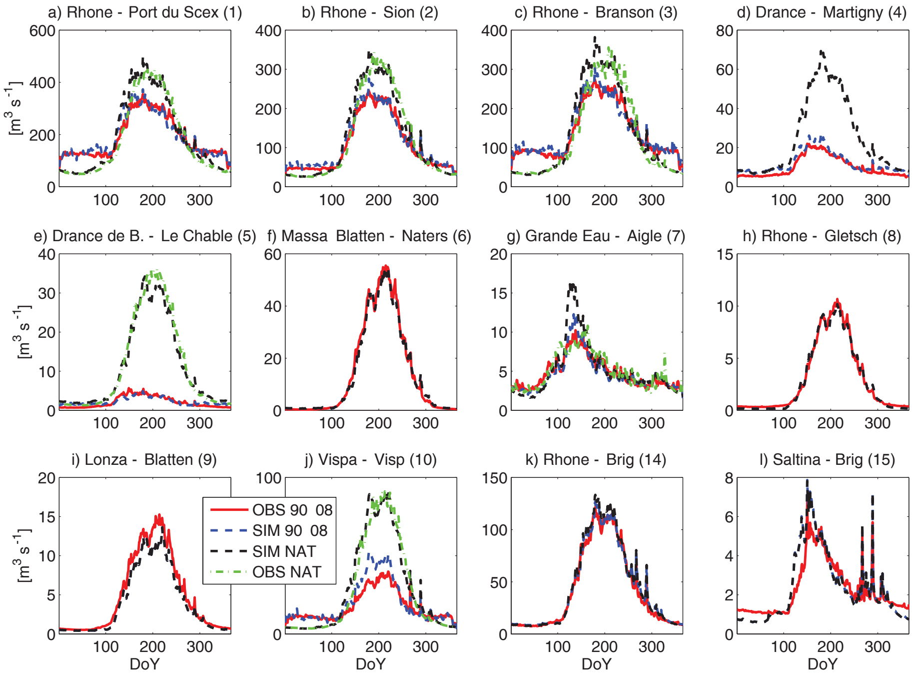

Fig. 4. Average seasonal cycles of streamflow in 12 river sections for the observations in the period 1990–2008 (red solid lines), for the simulations in the period 1990–2008 (blue dashed lines), for simulations of natural flow without anthropogenic influences in the period 1990–2008 (black dashed lines) and for observation in the "pre-dam" period (green dashed-dot lines). Observations before the construction of hydraulic infrastructure were available only for river section 1, 2, 3, 5, 7, and 10. In the river section 6, 8, 9, and 15 natural flow coincides with the simulation with all of the infrastructures.

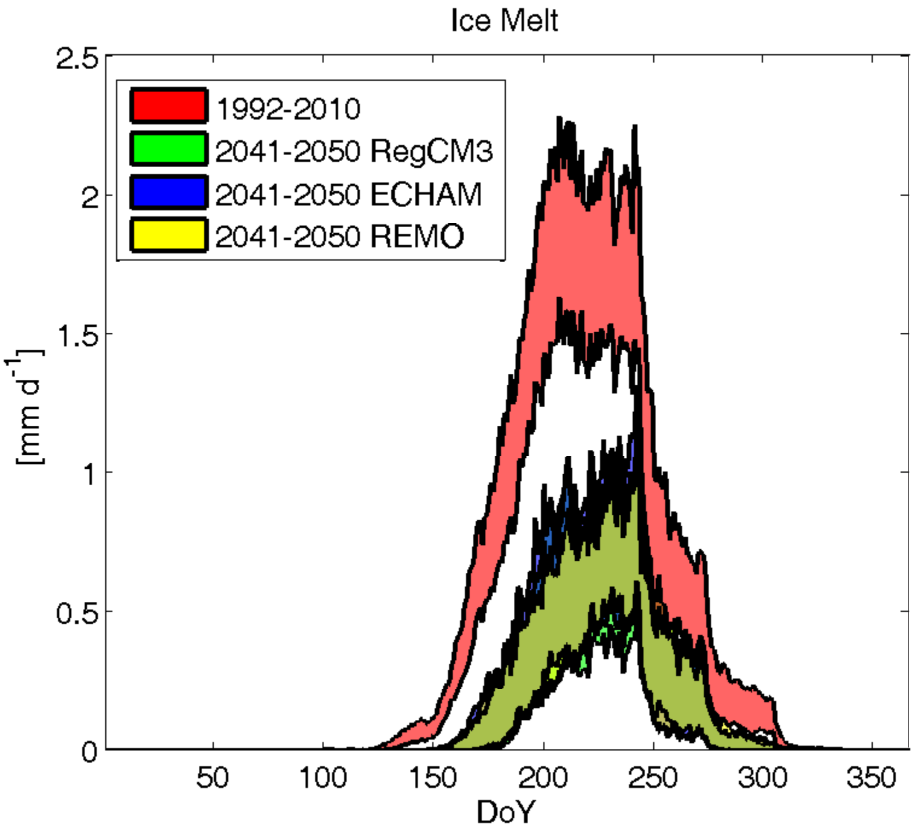

Fig. 5. A comparison among simulated annual cycles of ice melt averaged over the upper Rhone basin for the control scenario period 1992–2010, and future scenarios 2041–2050 for the stochastic downscaling driven by RegCM3, ECHAM5, and REMO. The colored bands include simulations within the 10 and 90 percentiles of the stochastic ensembles.

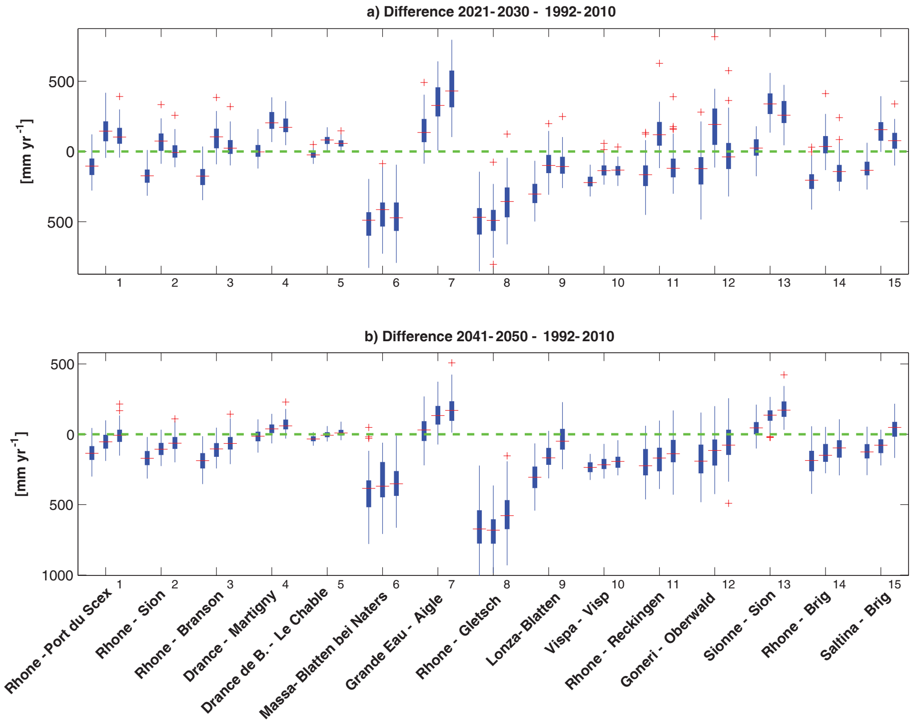

Fig. 6. Boxplots representing the difference in simulated streamflow [mm yr^{-1}] for the 15 river sections corresponding to the location of the streamgauges. The differences are between **(a)** the future period 2021–2030 and the control scenario 1992–2010; **(b)** the future period 2041–2050 and the control scenario 1992–2010. For each section the three boxplots indicate the stochastic downscaling driven by ECHAM5 (left), RegCM3 (central), and REMO (right).

Title Page
Abstract
Introduction
Conclusions
References
Tables
Figures
◀◀
▶▶
◀
▶
Back
Close
Full Screen / Esc
Printer-friendly Version
Interactive Discussion

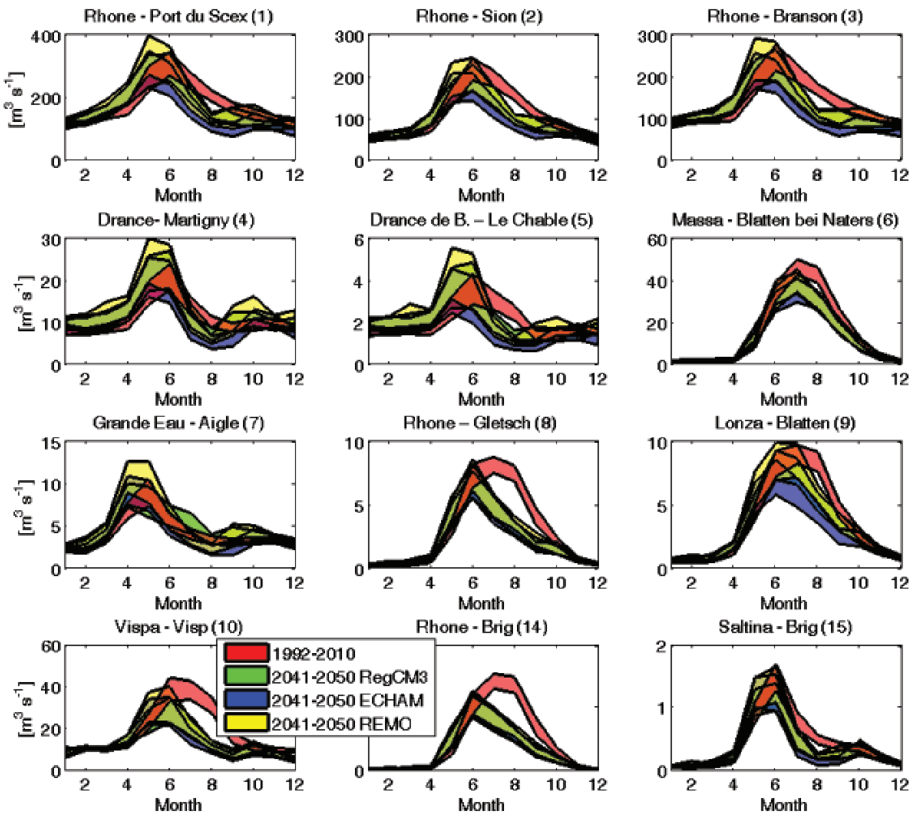

Fig. 7. A comparison among simulated annual cycles of streamflow [m^3 s^{-1}] for 12 selected river sections corresponding to the location of the streamgauges. The comparison is between the control scenario period 1992–2010, and future scenarios 2041–2050 for the stochastic downscaling driven by RegCM3, ECHAM5, and REMO. The colored bands include simulations within the 10 and 90 percentiles of the stochastic ensembles.

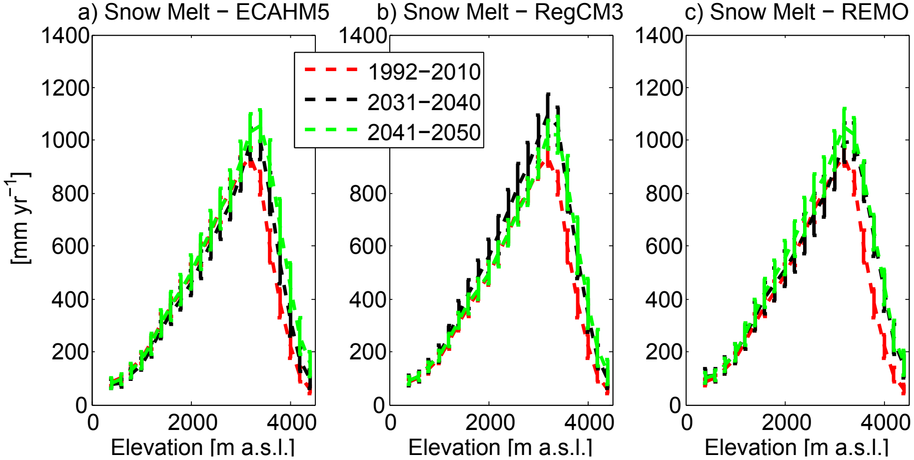

Fig. 8. A comparison between simulated snow melt for different elevation bands within the upper Rhone basin. The comparison is among the control scenario period 1992–2010 and the future scenarios 2031–2040 and 2041–2050 for the stochastic downscaling driven by ECHAM5 (subplot **a**), RegCM3 (subplot **b**), and REMO (subplot **c**). The vertical lines delineate the 10 and 90 percentiles of the stochastic ensembles.

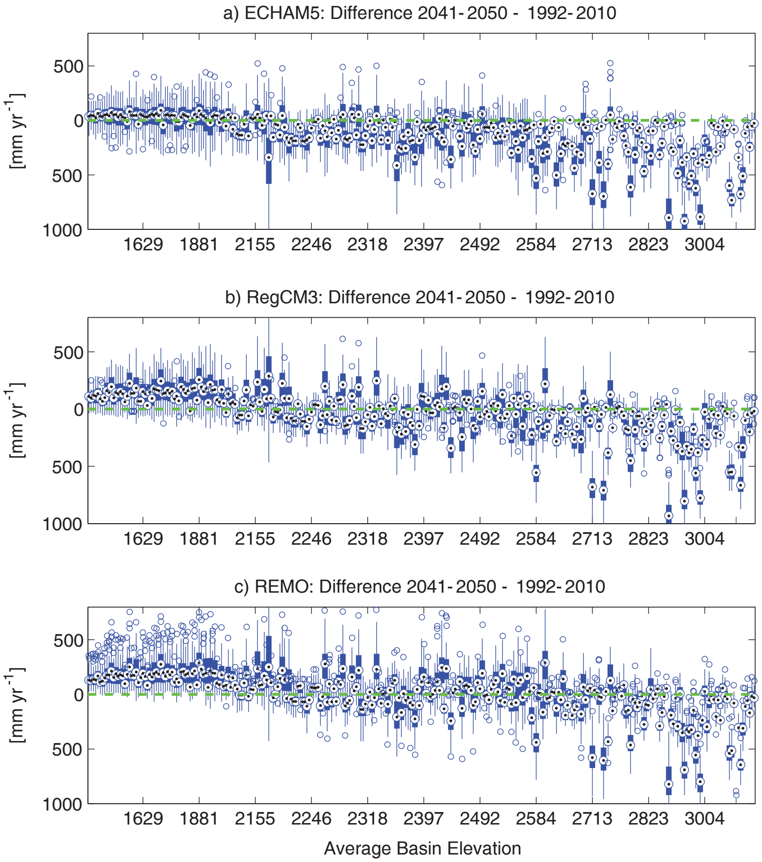

Fig. 9. Boxplots representing the difference in average simulated streamflow [mm yr^{-1}] between the future period 2041–2050 and the control scenario 1992–2010 for the 297 examined river sections ranked by the elevation of the upstream basin (contributing area). The difference are for the stochastic downscaling driven by ECHAM5 (subplot **a**), RegCM3 (subplot **b**), and REMO (subplot **c**).

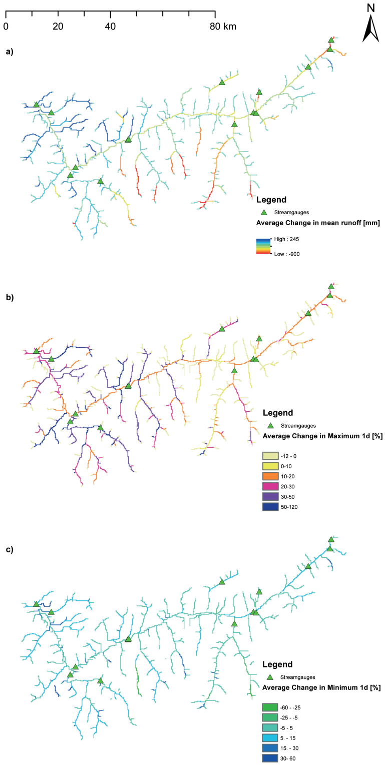

Fig. 10. The results of spatially-distributed changes between the future period 2041–2050 and the control scenario 1992–2010 in streamflow statistics for the stochastic downscaling driven by RegCM3 period. **(a)** Change in mean streamflow [$\mathrm{mm\,yr^{-1}}$]; **(b)** Change in daily maximum streamflow [%]; **(c)** Change in daily minimum streamflow [%].

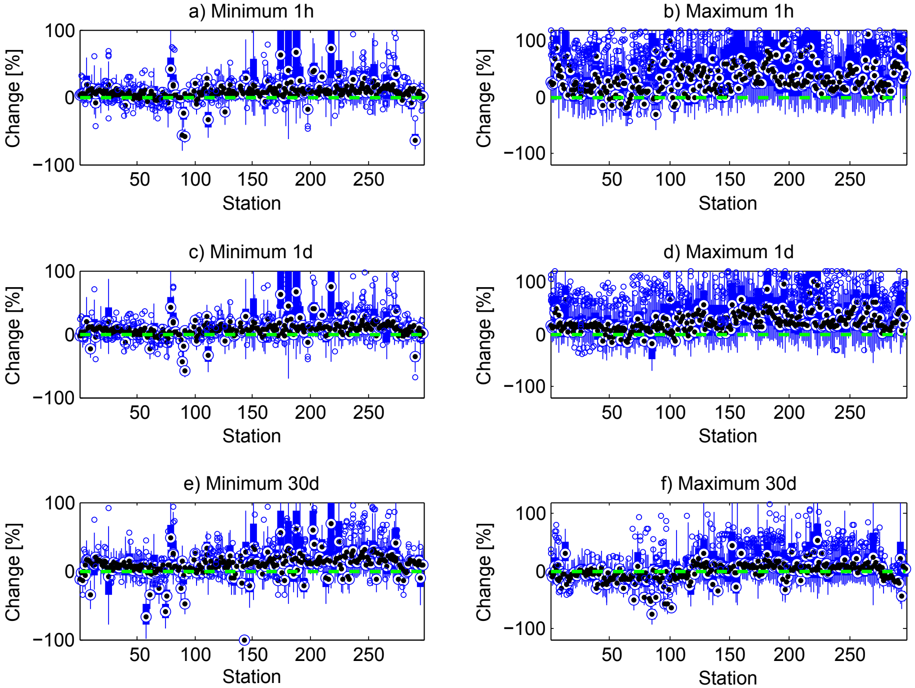

Fig. 11. Boxplots representing the difference for the stochastic downscaling driven by RegCM3 in minimum and maximum streamflow [%] between the future period 2041–2050 and the control scenario 1992–2010 for the 297 examined river sections. The difference are for minimum and maximum hourly (subplots **a** and **b**), daily (subplots **c** and **d**), and thirty days (subplots **e** and **f**) streamflow.

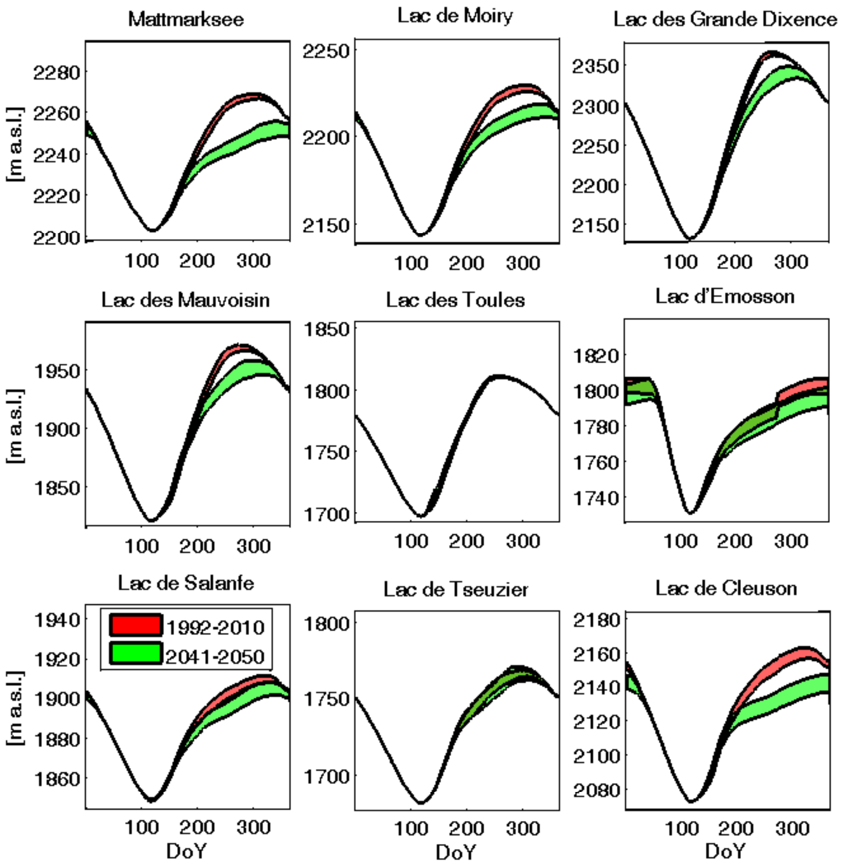

Fig. 12. A comparison among simulated annual cycles of reservoir levels [m a.s.l.]. The comparison is between the control scenario period 1992–2010, and future scenarios 2041–2050 for the stochastic downscaling driven by RegCM3. The colored bands include simulations within the 10 and 90 percentiles of the stochastic ensembles.